

Berichte

zur Polar-
und Meeresforschung

654
2012

Reports
on Polar and Marine Research



The Expedition of the Research Vessel "Polarstern"
to the Antarctic in 2012 (ANT-XXVIII/5)

Edited by
Karl Bumke
with contributions of the participants



ALFRED-WEGENER-INSTITUT FÜR
POLAR- UND MEERESFORSCHUNG
in der Helmholtz-Gemeinschaft
D-27570 BREMERHAVEN
Bundesrepublik Deutschland

ISSN 1866-3192

Hinweis

Die Berichte zur Polar- und Meeresforschung werden vom Alfred-Wegener-Institut für Polar- und Meeresforschung in Bremerhaven* in unregelmäßiger Abfolge herausgegeben.

Sie enthalten Beschreibungen und Ergebnisse der vom Institut (AWI) oder mit seiner Unterstützung durchgeführten Forschungsarbeiten in den Polargebieten und in den Meeren.

Es werden veröffentlicht:

- Expeditionsberichte
(inkl. Stationslisten und Routenkarten)
- Expeditions- und Forschungsergebnisse
(inkl. Dissertationen)
- wissenschaftliche Berichte der
Forschungsstationen des AWI
- Berichte wissenschaftlicher Tagungen

Die Beiträge geben nicht notwendigerweise die Auffassung des Instituts wieder.

Notice

The Reports on Polar and Marine Research are issued by the Alfred Wegener Institute for Polar and Marine Research in Bremerhaven*, Federal Republic of Germany. They are published in irregular intervals.

They contain descriptions and results of investigations in polar regions and in the seas either conducted by the Institute (AWI) or with its support.

The following items are published:

- expedition reports
(incl. station lists and route maps)
- expedition and research results
(incl. Ph.D. theses)
- scientific reports of research stations
operated by the AWI
- reports on scientific meetings

The papers contained in the Reports do not necessarily reflect the opinion of the Institute.

The „Berichte zur Polar- und Meeresforschung“
continue the former „Berichte zur Polarforschung“

* Anschrift / Address

Alfred-Wegener-Institut
für Polar- und Meeresforschung
D-27570 Bremerhaven
Germany
www.awi.de

Editor:

Dr. Horst Bornemann

Assistant editor:

Birgit Chiaventone

Die "Berichte zur Polar- und Meeresforschung" (ISSN 1866-3192) werden ab 2008 als Open-Access-Publikation herausgegeben (URL: <http://epic.awi.de>).

Since 2008 the "Reports on Polar and Marine Research" (ISSN 1866-3192) are available as open-access publications (URL: <http://epic.awi.de>)

The Expedition of the Research Vessel "Polarstern" to the Antarctic in 2012 (ANT-XXVIII/5)

**Edited by
Karl Bumke
with contributions of the participants**

**Please cite or link this publication using the identifier
hdl: 10013/epic.40370 or <http://hdl.handle.net/10013/epic.40370>**

ISSN 1866-3192

ANT-XXVIII/5

10 February - 15 May 2012

Punta Arenas – Las Palmas - Bremerhaven

**Chief scientist
Karl Bumke**

**Coordinator
Eberhard Fahrback**

Contents

1.	Zusammenfassung und Fahrtverlauf	3
	Summary and itinerary	5
2.	Weather conditions	6
3.	Sources and transformation of coloured dissolved organic material (CDOM) in Atlantic Ocean - Atlantic CDOM	9
4.	Autonomous measurement platforms for energy and material exchange between ocean and atmosphere (OCEANET)	21
5.	Chemical, physical and optical characterization of marine aerosols	24
6.	Composition and activity of the Bacterioplankton communities in a south-north transect of the Atlantic Ocean with a special emphasis on the Roseobacter clade and dissolved organic matter	30
7.	Higher trophic levels: distribution of marine mammals and seabirds at sea	36
8.	Measurement of the oxygen isotope anomaly (¹⁷O-excess) of ozone from 53°S to 53°N in the Atlantic marine boundary layer	39
9.	Culture experiments on the environmental controls of trace metal ratios (Mg/Ca, B/Ca, U/Ca) recorded in calcareous tests of Arctic deep-sea benthic foraminifera	43
10.	Molecular basis of climate sensitivity in Antarctic fish: mitochondrial functioning and its implication for ionic and osmotic regulation	44
11.	Sea trials and validation of the multibeam Hydrosweep DS-3	46
12.	Depth-profile of zirconium, vanadium, titanium and molybdenum in seawater-adsorption stripping voltammetry, an interesting analytical technique	50

13. Investigation of the numberdensity, properties and sources of ice nuclei in the marine atmosphere	54
14. Development of a web application for scientific devices and systems during ANT-XXVIII/5	56
15. References	59
APPENDIX	63
A.1 Teilnehmende Institute / participating institutions	64
A.2 Fahrtteilnehmer / cruise participants	66
A.3 Schiffsbesatzung / ship's crew	68
A.4 Stationsliste / station list PS 79	70

1. ZUSAMMENFASSUNG UND FAHRTVERLAUF

Karl Bumke

GEOMAR

Am 10. April 1012 begann der Fahrtabschnitt ANT-XXVIII/5 mit 44 Wissenschaftlern an Bord der *Polarstern* von Punta Arenas nach Bremerhaven. Zweck der Fahrt waren Untersuchungen atmosphärischer und mariner Parameter, der Transport von lebenden Fischen aus der Antarktis nach Bremerhaven, Untersuchungen zur Wechselwirkung von Ozean und Atmosphäre sowie Tests auf See von modifizierten Geräten. In Las Palmas ist ein Wissenschaftler abgestiegen und weitere 8 Fahrtteilnehmer sind aufgestiegen, darunter eine Lehrerin mit 3 Schülern.

Bereits auf dem Patagonischen Schelf fand die erste von insgesamt 36 Stationen statt. An den meisten Stationen wurden neben dem System bestehend aus CTD und Rosette auch ein optisches System für Unterwasserlichtmessungen eingesetzt sowie vom Schlauchboot aus Oberflächenwasserproben entnommen und eine weitere Messung von Unterwasserlicht durchgeführt (28 Stationen). Lediglich an einer dieser Stationen konnten wegen des Seegangs keine Messungen vom Schlauchboot aus durchgeführt werden. Daneben wurden an 5 Stationen Tests mit dem modifizierten Fächerecholot Atlas-Hydrosweep durchgeführt. Die guten Wetterverhältnisse ermöglichten, dass bis auf eine Einschränkung alle Messungen wie geplant durchgeführt werden konnten.

Die atmosphärischen Messungen umfassten die meteorologischen Standardparameter, die atmosphärische Strahlung, Aufnahmen der Bewölkung mit einer Wolkenkamera, die Turbulenz sowie die Vertikalprofile von Temperatur, Feuchte und Flüssigwasser. Die meisten dieser Messungen fanden in einem Messcontainer auf dem Helikopterdeck statt. Daneben befanden sich für luftchemische Untersuchungen, Schwerpunkt Aerosole, Kondensationskerne und Sauerstoffisotope, ein Aerosolcontainer und mehrere Luftsammler auf dem Peildeck.

Der Schwerpunkt der biologischen und chemischen Analysen der Wasserproben lag auf Untersuchungen von Bakterien vom *Roseobacter*-Stamm sowie auf dem Gehalt des Meerwassers an Spurenmetallen. Wasserproben wurden in der Regel aus den obersten 200 m der Wassersäule entnommen, an 11 Stationen wurden auch Tiefen bis zu 5600 m beprobt. Analysen des Gehalts an Phytoplankton wurden mit Hilfe von Unterwasserstrahlungsmessungen durchgeführt, wo aus der Absorption Licht bestimmter Wellenlängen Rückschlüsse auf den Gehalt verschiedener Bestandteile des Meerwassers gezogen werden können. Der andere Teil der Unterwasserlichtmessungen zusammen mit gleichzeitigen Messungen der Strahlungsverhältnisse an der Wasseroberfläche dient der Untersuchung der Eindringtiefe von Strahlung in den Ozean.

Die ozeanographischen Messungen werden auf einen möglichen Zusammenhang mit den auch auf dieser Fahrt beobachteten Populationsdichten von Seevögeln und Meeressäugern hin untersucht.

Am 15. Mai erreichte *Polarstern* Bremerhaven.

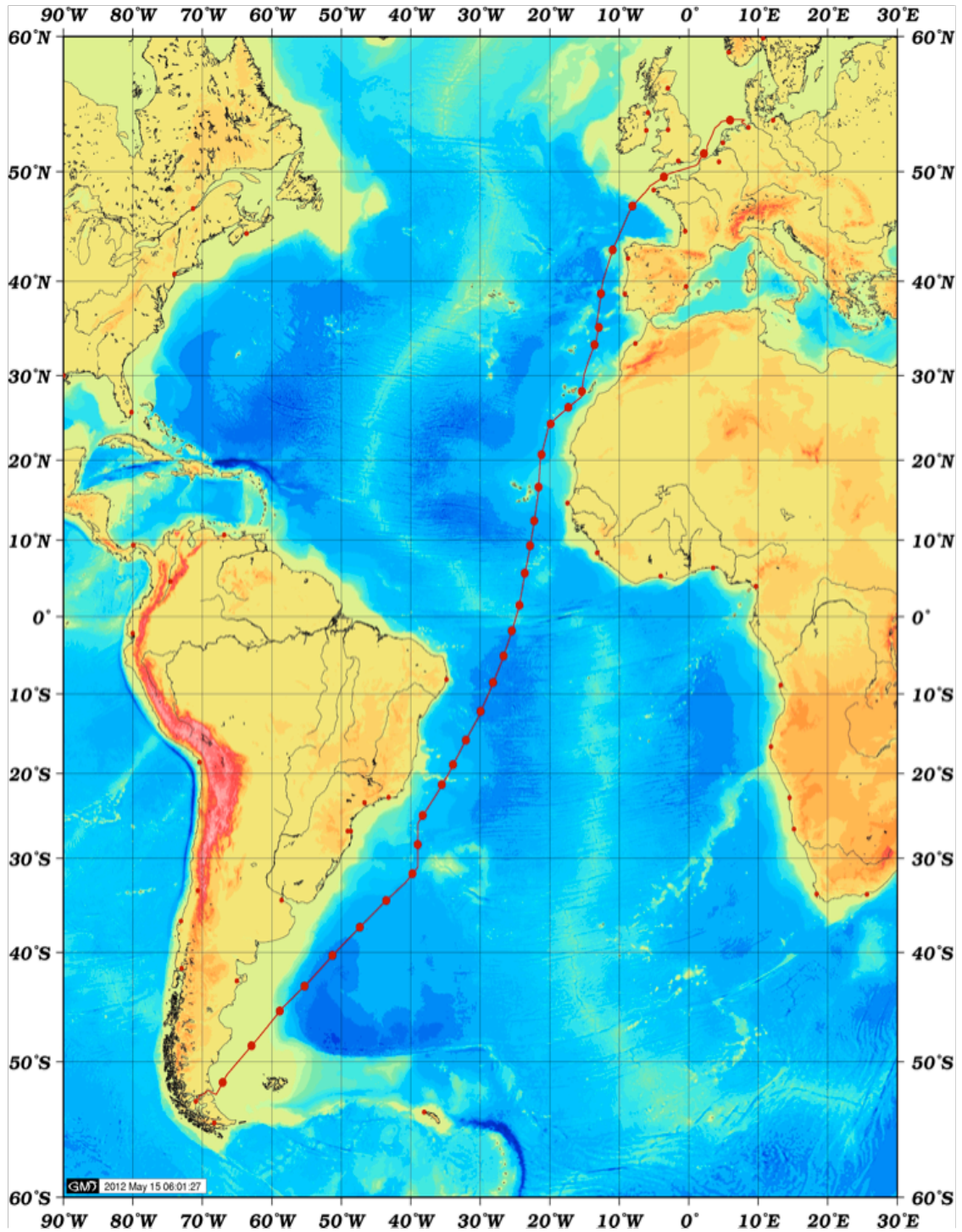


Fig. 1.1: Kurs der Polarstern-Reise ANT-XXVIII/5
Cruise track of Polarstern during the expedition ANT-XXVIII/5

SUMMARY AND ITINERARY

On April 10 at 6.00 pm *Polarstern* started in Punta Arenas for the ANT-XXVIII/5 cruise toward Bremerhaven with 44 scientists on board. The cruise was utilized for investigations of atmospheric and marine properties, transport of living Antarctic fish to Bremerhaven, sea acceptance tests of modified instruments as well as for ocean and atmosphere interaction. In Las Palmas, one scientist disembarked and another eight participants came on board, among them a teacher and three pupils.

Already on the Patagonian shelf, the first of 36 stations took place. At the majority of the stations a CTD equipped with a rosette was deployed. Additionally, an optical system measured underwater radiation and the zodiac was used to collect surface water probes and to perform an additional measurement of underwater radiation (28 stations). At only one station did no zodiac measurements take place due to rough seas. Beside the performance of the modified multi-beam echo-sounder Atlas hydrosweep was tested at 5 stations. Pleasant weather conditions allowed that, except for one constraint, all measurements were carried out as planned.

Atmospheric measurements comprised meteorological standard parameters, turbulence, radiation, monitoring of cloudiness and aerosol in the atmosphere, and the tropospheric state with respect to temperature, humidity, and liquid water content. Some of the measurement systems were installed in a measurement container on the helicopter deck. For purposes of air chemistry and monitoring of aerosols, condensation nuclei, and oxygen isotopes, an aerosol container and several air samplers were placed on the monkey deck.

Biological and chemical analyses of seawater were focused on investigations regarding bacteria of the *Roseobacter* clade, and beside others, the concentration of trace metals. Water samples were usually taken from the upper 200m of the water column. At 11 stations water probes were collected up to depths of about 5,600m. Additionally, spectral underwater light measurements were carried out which allow for an estimation of the concentration of phytoplankton and other matters by an analysis of the portion of absorbed light.

Underwater light measurements by the second system, handled onboard the zodiac, together with simultaneous measurements of radiation fluxes at the sea surface, gave information about the penetration depth of light in the ocean.

The oceanographic measurements will be investigated to detect the mechanisms underpinning the distribution of sea birds and marine mammals, which were also observed during this cruise.

On May 15 *Polarstern* arrived in Bremerhaven.

2. WEATHER CONDITIONS

Max Miller, Juliane Hempelt

DWD

On Tuesday, April 10 2012 (6:00 pm), *Polarstern* left Punta Arenas for the campaign ANT-XXVIII/5 at moderate northerly wind. A storm west of the Drake Passage moved towards the Antarctic Peninsula and we got at its northern edge for a short while. Therefore the north-easterly wind increased up to Bft 7 as we passed the Strait of Magellan during the night to Wednesday. While sailing northeast *Polarstern* departed from the storm. The Wind abated and veered southwest.

On Friday (April 13) a new storm over the Pacific approached the Drake Passage and *Polarstern* temporarily got at the outer edge of this storm. The north-westerly wind increased up to Bft 7 for short times and veered southwest in the evening while a weak cold front crossed our track. During the night to Saturday the wind abated to 4 to 5 Bft again and clouds broke up.

Off Uruguay a high formed and moved east. On Tuesday (April 17) we reached its centre at sunshine and mostly calm conditions. Afterwards we measured easterly wind around 4 Bft at the north side of the high and the swell didn't exceed 1.5 m. A weak trough off Brazil caused isolated showers and on Tuesday (April 24) *Polarstern* entered the trade wind zone. The wind veered southeast and increased up to Bft 6 on Thursday (April 26) at a swell around 2 m.

While approaching the intertropical convergence zone (ITCZ) on Friday evening (April 27) the wind veered east and abated to Bft 4. Some showers occurred but thunderstorms didn't cross the ship's route.

On Monday (April 30) we entered the northeast trade wind zone. The wind gradually increased and reached Bft 7 for a while on Wednesday (May 2). At the same time we sailed a large area filled with dust from the Sahara. We temporarily measured a visibility less than 10 km and the sun seemed to be behind frosted glass. Due to the haze no clouds could be observed. Approaching the Canary Islands the trade winds abated and the dust vanished.

Sunday morning (May 6) *Polarstern* reached Las Palmas at light wind from north. Already at noon we continued our cruise. A high extended from the Canary Islands to the western part of the Mediterranean Sea and *Polarstern* crossed its centre. Therefore we measured only light and variable winds on the first part of our way north.

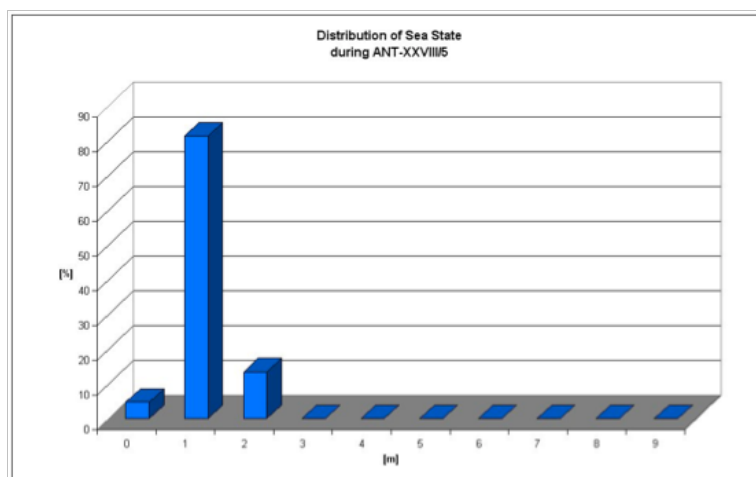
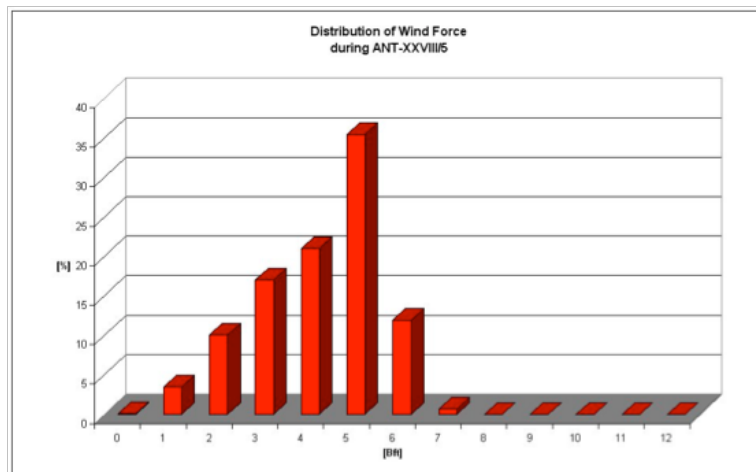
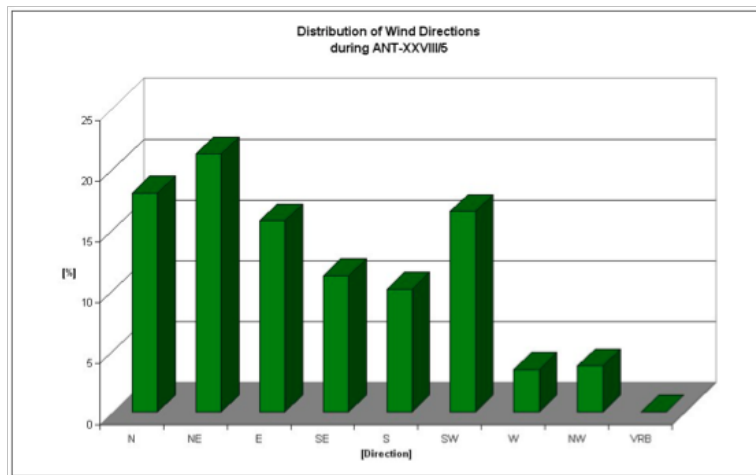


Fig. 2.1: Statistics of wind directions, wind force, and wave heights for the cruise leg ANT-XXVIII/5

Off the Iberian Peninsula we reached the southern edge of a weakening low which moved from the Atlantic towards Great Britain. Wind from south to southwest increased for short times up to Bft 6 on Wednesday (May 9) and abated again on Thursday. Meanwhile a high over the Atlantic had built a ridge towards the Bay of Biscay. On Friday (May 11) the wind veered northeast within the Bay of Biscay and increased up to Bft 6 at a swell of 1.5 to 2 m. This high moved on towards Ireland. Passing the western part of the English Channel *Polarstern* sailed near its centre. Thus the wind calmed down during the night to Sunday (May 13th).

At the same time a storm had reached a position between Iceland and Scotland and moved towards Norway. On Sunday afternoon we got at its southern edge while sailing the eastern exit of the Channel. The south-westerly wind freshened up to Bft 5. During the night to Monday the wind reached its maximum at Bft 6 to 7 and the swell increased up to 2 m. On Monday a secondary low formed over the North Sea. Operating close to its centre caused a decrease of wind and waves.

Around noon on Tuesday, May 15 2012, *Polarstern* reached Bremerhaven on schedule at southerly wind Bft 4 to 5. The statistics of wind direction and force as well as of sea state are summarized in Fig. 2.1.

3. SOURCES AND TRANSFORMATION OF COLOURED DISSOLVED ORGANIC MATERIAL (CDOM) IN ATLANTIC OCEAN - ATLANTIC CDOM

Piotr Kowalczyk¹, Sławomir Sagan¹, Monika Zabłocka¹, Anna Raczkowska², Oskar Głowacki² ¹IOPAS
²University of Gdańsk

Objectives

The scientific objectives of the IOPAS project were:

- identify individual CDOM components characterize them by spectral properties of excitation/emission fluorescence and absorption
- identify processes that control distribution of specific component in time and space and find those component, which distribution is controlled by physical conservative mixing of water masses with distinctly different optical and hydrological properties
- derive empirical relationships between specific CDOM components and inherent and apparent optical properties of marine waters and salinity
- derive empirical relationships between spectral properties of CDOM fluorescence and absorption with DOC concentration. Investigate the temporal and spatial variability of $a_{\text{CDOM}}/\text{DOC}$ and FDOM/DOC .
- establish the zonal variation of the depth integrated action spectra (the product of the CDOM absorption spectrum and spectral distribution of underwater irradiance at given depth) of the CDOM photo degradation.

Work at sea

Measurements of inherent optical properties of water samples

Water samples for determining CDOM absorption, particulate absorption, CDOM fluorescence, chlorophyll *a* concentration and DOC concentration were collected at fixed depths with Niskin bottles attached at to CTD rosette during solar noon casts. Water samples depths were determined upon features of the vertical profiles of the chlorophyll *a* fluorescence: at all stations following depths were sampled: 300 m, 200 m, 100 m or Deep Chlorophyll Maximum (which ever deeper), bottom of the mixed layer, middle of the mixed layer. The surface water was collected from zodiac motor boat with use pre-rinsed beaker and transferred to 10 liter HDPE container. Additionally water samples from deep ocean were collected for determining CDOM absorption, CDOM fluorescence and DOC concentration.

Water samples for determination of CDOM absorption, fluorescence EEM and DOC concentrations underwent a two-step filtration process immediately after collection. The first filtration was through acid-washed Whatman glass fiber filters (GF/F, nominal pore size 0.7 μm). The particulate material retained on filters was stored for further laboratory measurements of particulate absorption and chlorophyll *a* concentration. That analysis will be done at laboratory on land in the Institute of Oceanology, Polish Academy of Sciences, Sopot, Poland. The chlorophyll *a* concentration will be determined using the spectrophotometric method (HELCOM, 1988). The particulate matter retained on the filters will be extracted for 24 h in 96 % ethanol. The absorbance of the extract will be measured with use of the Perkin-Elmer Lambda 650 dual beam UV-VIS spectrophotometer. The following equation will be used to convert the absorbance at 665 nm to chlorophyll *a* concentration:

$$\text{Chl}[\text{mg m}^{-3}] = 10^3(D_{665} - D_{750})\nu 83^{-1}r^{-1}V^{-1} \quad (1)$$

Here D_{665} is the absorbance at 665 nm (after correction for blank ethanol), D_{750} the absorbance at 750 nm (after correction for blank ethanol), ν the volume of ethanol (ml), r the cell (cuvette) path length (cm), V the volume of filtered seawater (l), and 83 ($\text{l g}^{-1} \text{cm}^{-1}$) is the chlorophyll *a*-specific absorption coefficient in ethanol (Schotz, 1962).

The spectral absorption coefficient of particulate matter, $a_p(\lambda)$, will be estimated derived from filter-pad measurements using a dual-beam^p Perkin-Elmer Lambda 650 spectrophotometer equipped with the integrating sphere. First, an appropriate volume of seawater (0.5–2 L depending on particle concentration in water) was filtered onto a 25-mm glass-fiber filter (GF/F). Filters were preserved and stored deep frozen for further analysis in laboratory. The absorption spectrum of particles, $a_p(\lambda)$, retained on a filter will be determined using the transmittance-reflectance (T-R) spectrophotometric method (Tassan and Ferrari, 1995). Transmittance and reflectance will be measured in spectral range between 380 and 750 nm with a 1 nm resolution. A formula derived by (Kaczmarek et al., 2003) will be applied for correction for path length amplification factor (β).

Measurements of optical properties of CDOM

Portion of the filtered water was then passed through Sartorius 0.2 μm pore cellulose membrane filters to remove fine-sized particles. This water was used for spectrophotometric and spectrofluorometric scans for determination of CDOM absorption spectra, CDOM fluorescence Excitation-Emission Matrix spectra, and the DOC concentration. Spectroscopic analysis has been done in the laboratory on board *Polarstern*.

The absorption of light by CDOM can be parameterized as an exponential function as follows:

$$a_{\text{CDOM}}(\lambda) = a_{\text{CDOM}}(\lambda_{\text{ref}}) * e^{-S(\lambda - \lambda_{\text{ref}})} + K \quad , \quad (2)$$

where $a_{\text{CDOM}}(\lambda)$ is the absorption coefficient at wavelength λ (m^{-1}), λ_{ref} is a reference wavelength, and S is the CDOM absorption spectrum slope parameter coefficient (nm^{-1}). K is a background constant that allow any baseline shift caused

3. Sources and transformation of CDOM in Atlantic Ocean

by residual scattering by fine size particle fractions, micro-air bubbles or colloidal material present in the sample, refractive index differences between sample and the reference, or attenuation not due to organic matter.

Spectral absorption by CDOM was measured immediately after water filtration, in the laboratory on board *Polarstern* using a double-beam Perkin-Elmer Lambda-35 spectrophotometer with a 10-cm quartz cell in the spectral range of 200–700 nm. Milli-Q™ water was used as the reference for all measurements. The absorption coefficient $a_{\text{CDOM}}(\lambda)$ was calculated using the following equation:

$$a_{\text{CDOM}}(\lambda) = 2.303 * \frac{A(\lambda)}{L} \quad (3)$$

where $A(\lambda)$ is the absorbance (optical density) and L the path length.

The spectra of the CDOM absorption coefficient were used to calculate the CDOM absorption spectrum spectral slope coefficient with use of the non-linear regression technique (Stedmon et al., 2000) at 3 different spectral ranges: 275 - 295 nm, 350 - 400 nm and 300 - 650 nm. The spectral slope coefficients $S_{275-295}$ and $S_{350-400}$ were used to calculate the slope ratio S_R according to Helms et al., (2008), which is a the ratio of $S_{275-295}$ to $S_{350-400}$. The slope ratio S_R is an indicator of molecular weight, source, and photobleaching of chromophoric dissolved organic matter.

Samples for fluorescence were treated in the same manner as those for absorption measurements. Before spectroscopic scans of DOM, the samples were allowed to warm to room temperature. DOM fluorescence measurements were made on a Varian Cary Eclipse scanning spectrofluorometer. A series of emission scans (280 - 600 nm, 2 nm resolution) were collected over excitation wavelengths ranging from 240 to 500 nm by 5-nm increments. The instrument was configured to collect the signal using maximum lamp energy and 5 nm band pass on both the excitation and emission monochromators. Collected Excitation Emission Matrix spectra will be further processed using DOM fluorescence toolbox developed by Stedmon and Bro (2008). Samples will be spectrally corrected with set of instrument dependent correction coefficients and calibrated against the water Raman scatter peak (excitation wavelength of 350 nm) of a Milli-Q™ water sample, run the same day. Then a Raman normalized Milli-Q™ EEM will be subtracted from the data to remove the Raman signal. The Raman normalization and correction procedures will result in spectra that are in Raman units (R.U., nm⁻¹) and are directly comparable to corrected spectra measured on other machines. The corrected and calibrated EEM spectra will be statistically analysed with the method described by Stedmon et al., (2003), and the PARAFAC model will be derived with use of the in MATLAB using the "N-way toolbox for MATLAB ver. 2.0"(Andersson and Bro, 2002). PARAFAC aids the characterization of fluorescent DOM by decomposing the fluorescence matrices into different independent fluorescent components.

DOC concentration

Samples for DOC measurements were passed through 0.2 µm pre-cleaned membrane filters. A total of 40 ml aliquots of filtrate were acidified with 150 µl 0.1 M HCl and stored in the dark at 4° C until laboratory analysis. Samples will be

shipped in the conditioned container to Institute of Oceanology, Polish Academy of Sciences, Sopot, Poland for estimation of the DOC concentration in the laboratory. These will be done in a 'HyPerTOC' analyser (Thermo Electron Corp., The Netherlands) using UV/persulphate oxidation and non-dispersive infrared detection (Sharp 2002). Measurements of each sample using the standard addition method (potassium hydrogen phthalate) will be performed in triplicate. Quality control of DOC concentrations will be performed with reference material supplied by Hansell Laboratory, University of Miami. The methodology will ensure satisfactory accuracy. The quality assessment performed in the previous studies in the Baltic Sea has given following results: average recovery 95 %; $n = 5$; CRM = 44 – 46 $\mu\text{M C}$; our results = 42 – 43 $\mu\text{M C}$ and precision characterized by a relative standard deviation (RSD) of 2 % (Kowalczyk et al., 2010).

Underway and vertical profiles optical measurements of spectral attenuation and absorption coefficients, CDOM fluorescence and particles size distributions

In addition to collecting water samples for laboratory spectroscopic measurements of inherent optical properties of the sea water, inherent optical properties were also measured *in-situ*, along the ship track, using Integrated Optical-Hydrological Probe. The Integrated Optical-Hydrological Probe was also deployed to record the vertical distribution of inherent optical properties at each station starting from April 13, 2012 and finished at May 11, 2012.

The TRIOS MicroFlu-CDOM and TRIOS MicroFlu-Chla fluorometers and Sea-Bird Electronics SBE 49 FastCAT CTD were coupled with the WET Labs Inc. ac-9 plus spectrophotometer, which functioned as the data integrator. The instrument setup, referred to as the Integrated Optical-Hydrological Probe, was fitted into one rig and connected by telemetry cable with the power supply and data transmission and control deck unit (for underway operation mode) or was powered from a battery, logging data internally for vertical profiling. The ac-9 plus and CTD water intakes were installed on the same horizontal plane as the optical window of the fluorometer. The data from instruments were merged and synchronized along with their time stamps with WAP 4.25 software supplied by the WET Labs. All of the signals were processed further using software written in the Matlab ® environment. This had calibration procedures for all the sensors, and it merged all the measured geophysical parameters and calibrated values in physical units into a depth binned matrix.

The Integrated Optical-Hydrological probe was deployed as the quasi-flow through instrument for continuous underway measurements of inherent optical properties of sea water. It was placed in the tank filled with flowing water pumped from the ships non-toxic water supply system. The retention time of water present in the tank was estimated for ca. 3 minutes. Assuming an average ship cruising speed for 10 knots and average retention time of water in the tank, this gives ca. 900 m spatial displacement between place where water volume was taken by the non-toxic water supply and actual ships position during measurement time in the tank. The underway measurements of inherent optical properties started on April 12, 2012 and were continued until May 12, 2012. All optical elements of the sensors were routinely cleaned every 24 h. Apart of that, maintenance and field calibration procedures recommended by manufactures were applied. During the

3. Sources and transformation of CDOM in Atlantic Ocean

whole deployment period readings from instruments were monitored continuously for bio-fouling effects; no anomalous readings were noticed.

The inherent optical properties of the sea water were measured using an ac-9 plus (WET Labs Inc., USA) spectral attenuation and absorption meter. *In-situ* measurements of the light absorption a and attenuation c were performed at wavelengths of 412, 440, 488, 510, 532, 555, 650, 676 and 715 nm. The instrument was calibrated in pure water and routinely checked for stability with air-readings. Air and water offsets, temperature and salinity corrections were applied according to the manual. Since the ac-9 absorption signal needs correction for scattering, the so-called 'Zaneveld method' was applied, which assumes zero absorption for 715 nm (Zaneveld et al. 1994).

CDOM fluorescence was measured with a MicroFlu-CDOM fluorometer (TRIOS GmbH, Germany), which is suitable for *in-situ* measurements without the prior filtration of the water. The MicroFlu-CDOM fluorometer uses UV-LED in pulse mode as the excitation light source. The maximum of the excitation light spectrum is 370 nm. A small percentage of light is reflected by the dichroitic beam splitter and is used as the reference signal for calculating the excitation energy. The fluorometer excites samples of a small volume of water at the front of the optical window at a focal length of 15 mm. It uses a photo-diode with an interference filter as the light detector. The maximum emission of the light detector is set at 460 nm. Specially developed circuitry eliminates the influence of ambient light. The MicroFlu-CDOM fluorometer was calibrated by the manufacturer annually during the deployment period (2008–2012). The measured signal was transmitted to the via telemetry cable to a deck power supply and telemetry control unit in the form of the analog DC voltages. The voltages were converted to QSE calibrated units, as described in details by Kowalczyk et al. (2010). The TRIOS MicroFlu-Chla fluorometer has the same functional features the one for CDOM measurements except different excitation, (470 nm), and emission (685 nm), wavelengths. The TRIOS MicroFlu-Chla fluorometer was factory calibrated in chlorophyll a concentration units – $\mu\text{g l}^{-1}$.

The laser *in-situ* scattering and attenuation meter LISST 100X (Sequoia Instruments, Inc., USA) was deployed along with the Integrated Optical-Hydrological probe for continuous underway measurements of particle size distribution. This instrument was equipped with flow through measurements chamber fed with the marine water from the ship's non-toxic water supply system. This self-contained instrument consists of the a solid-state laser operating at 670 nm wavelength and fiber-optically connected to a laser beam collimating system, a beam manipulation and orienting system, a scattered-light receiving lens, the specially designed 32-ring detector, preamplifier electronics, a ring-selecting multiplexer circuitry, and a data logger. The principal measurement — angular scattering distribution — is obtained over 32 ring-detectors whose radii increase logarithmically from 102 to 20,000 microns. The detector is placed in the focal plane of the receiving lens. The rings cover an angular range from 0.0017 to 0.34 radians. This angular range corresponds, respectively, to size ranges from 1.2 to 250 microns. The laser diffraction method for sizing particles is used for determining size distribution for the simple reason that for laser diffraction, the composition or refractive index of the particles is not important. This method determines size distribution of an ensemble of particles, as opposed to counting type devices that size one particle at a time (Agrawal et al., 2008). The cleaning, maintenance and field calibration schedule was the same as for the Integrated Optical-Hydrological probe.

The inherent optical properties spectra collected during the underway and vertical profiles deployments of the Integrated Optical-Hydrological probe would require the post cruise reprocessing, since the instruments have been operating nearly at limits of their characteristics due to extreme clear waters. This will include close inspection of potential spikes and unusual features in spectral distribution of the absorption coefficient and attenuation coefficient spectra.

Underway above water radiometric measurement

The daily radiometric measurement was performed to contribute to the calibration-validation effort of ocean color satellite imagery products. The free of atmospheric error, water-leaving radiance, sky radiance and downwelling irradiance were measured from the port side of "monkey deck" of the *Polarstern*. Measurement was conducted along ship track in day light between 09:30 and 17:30 local time, daily. The measurements were not conducted when the ship was stopped on station, around the local solar noon except recording the intensity of incident solar irradiance, needed as the reference for underwater profiling radiometer. Measurements started on April 14, 2012 and were conducted every day until May 11, 2012. The measurements were suspended on April 19, 2012, April 29, 2012, and May 1, and 2, 2012, and 10 May, 2012, due to adverse weather conditions: rain events or passing through heavy seas, which resulted of generation of thick foam by the ship's hull. The sensors were calibrated in air and rain droplets on the optical lenses and cosine collector of irradiance sensor change the radiometers readings and deteriorate their accuracy.

The measurement system consists of set of RAMSES hyperspectral radiometers manufactured by TRIOS Optical Systems, TRIOS GmbH, Germany: a down-looking radiance radiometer, a sky-viewing radiance radiometer, downwelling irradiance radiometer. All radiometer were calibrated at the manufacturer laboratory on annual basis. All radiometers were mounted on the bow platform in the specially designed deployment rig that enabled the angular adjustments in the vertical (nadir) and horizontal (azimuth) planes. Radiometers were connected with the deck unit telemetry control and the power supply deck unit, which was linked with the laptop computer through the RS232 serial port. The measurements were controlled by the MSDA_ex software. All radiometers were measuring radiometric quantities simultaneously triggered by the software trigger every 20 s. The data were collected in the spectral range from 350 nm to 850 nm with 2 nm resolution. The signal integration time varied from 6 ms to 128 ms depending on the illumination conditions by the incident solar radiation. These data were then used to estimate normalized water-leaving radiance as a function of wavelength. The radiance detector was set to view the water at 45 degrees from nadir as recommended by Mueller et al. (2003b). Sensors were rinsed regularly with Milli-Q™ water in order to remove salt deposits and any dust. The water radiance radiometer was able to view over an azimuth range of ~90 degrees across the ship's heading with no contamination from the ship's wake. The direction of the sensor was manually adjusted every hour to view the water between 90 - 120 degrees range from the sun's azimuth, to minimize sun glint. Protocols for operation and calibration were performed according to Mueller (Hooker et al., 2003; Mueller et al., 2003a; Mueller et al., 2003b). The collected data set will require post-cruise reprocessing for removing possible signal contamination by foam on the seas surface (generated by ship's hull, or breaking wave during the rough sea conditions). The reprocessed signal will be used to calculate the spectral remote sensing values.

In water radiometric measurement with use of the profiling radiometer

Every day, close the solar noon in local time, from April 12, 2012 until 11 May 2012, vertical profiles of spectral underwater radiation were recorded with use of profiling underwater free fall radiometer – the Compact Optical Profiling System COPS, (Biospherical Instruments Inc., San Diego, USA). On April 26, 2012, the Compact Optical Profiling System was not deployed due to adverse weather conditions. This small instrument consist with the submersible radiometer that measures the solar radiation at 12 spectral bands: 305, 320, 340, 380, 412, 443, 490, 555, 625, 665, 683, 710 nm, and E_d PAR, tilt and roll, temperature and pressure sensors attached to profiling vehicle connected with telemetry cable with the deck power supply and telemetry control unit and is manually deployed over board the zodiac. This instrument measures the intensity of the solar radiation that propagates through the water column into a deep in the function of depth and wavelength. The measurements of underwater light field were consistent with The Ocean Optics Protocols (Mueller et al., 2003b). Manual deployment of this instrument from zodiac was necessary for several reasons: sailing away from *Polarstern* we could avoid the ship shadow and disturbances of the light field caused by foam generated by ships propellers and thrusters and waves braking on the ship's hull. We can also eliminate the risk that the instrument would be entangled in to propeller or thruster and damaged. Before each deployment the pressure sensor was tarred to adjust its reading to changes of atmospheric pressure. The descent rate was usually maintained with range 0.4 m/s. During the COPS deployment the incident solar irradiance intensity was measured with use of the TRIOS Ramses radiometer mounted on the *Polarstern's* "monkey deck". All profiles of $E_d(z, \lambda)$ and above-water measurements of $E_s(\lambda)$ were graphed and carefully examined as a quality check. All measurements in which significant and rapid changes in the ambient light occurred during vertical profiling, and any peculiar spectra will be eliminated from further analysis. The diffuse attenuation coefficient for downwelling irradiance at the 12 spectral bands and PAR spectral range, $K_d(z, k)$, $K_d(\text{PAR})$ will calculated from the log-transformed $E_d(z, k)$ and $E_d(z, \text{PAR})$ based on a well-established methodology (Smith and Baker, 1984).

Expected results

Our measurements enable us to measure light intensity and its spectral quality at given depths and that way we can estimate how quickly light is diminished in the ocean, and which part of the solar radiation spectrum penetrate deepest. The light conditions in the deep are essential for phytoplankton to grow and produce the biomass in the process of photosynthesis. We were particularly interested in penetration of the UV radiation in to the ocean's depths. This part of solar radiation spectrum is harmful for marine organisms but also it interacts with particulate and soluble material contributing to its degradation through photoreactions. Fig. 3.1 presents the distribution of downwelling spectral irradiance in the function of depth in selected spectral bands at selected stations during the cruise.

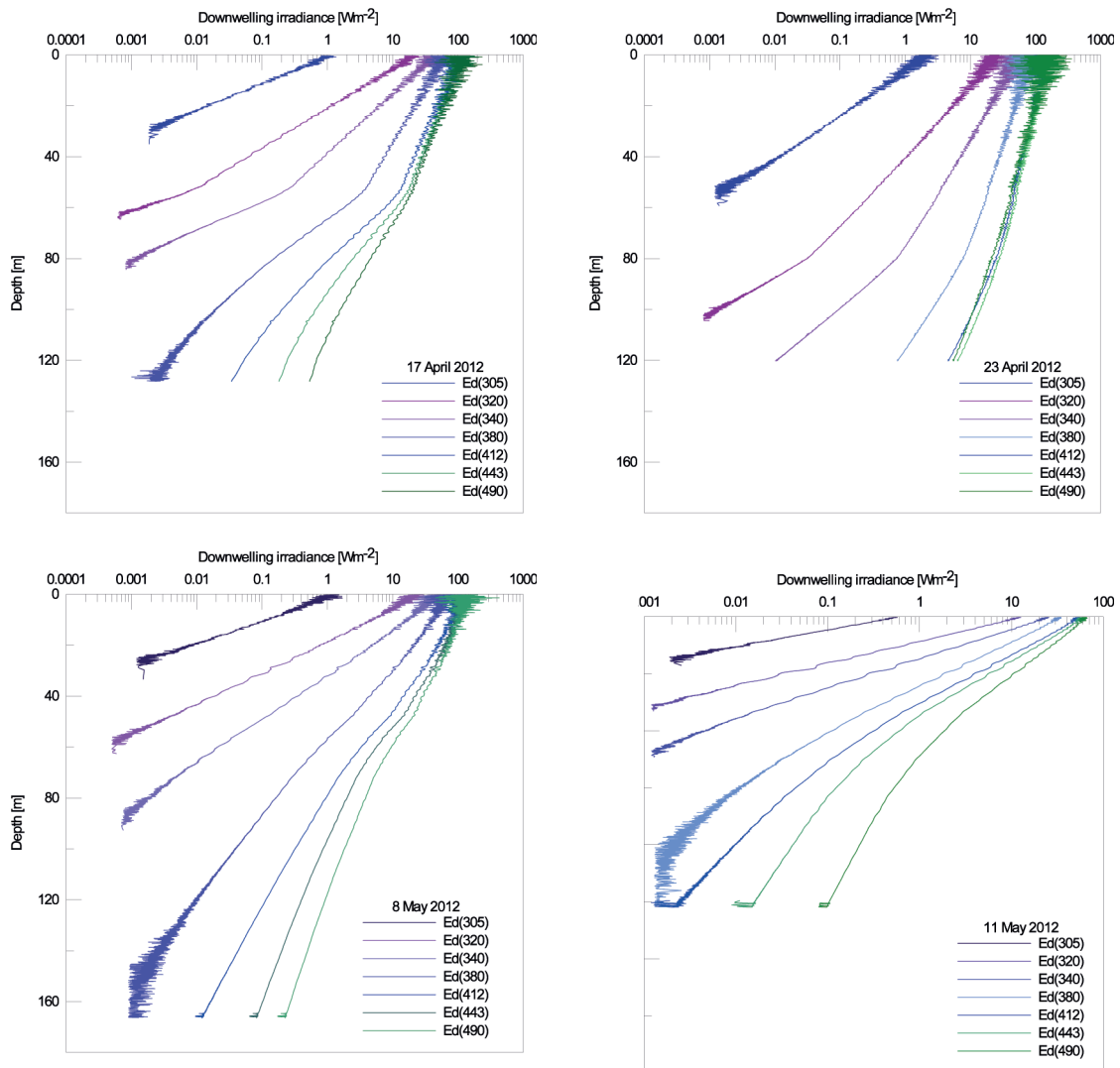


Fig. 3.1: Distribution of downwelling spectral irradiance in the function of depth in 7 spectral channels: 305, 320, 340, 380, 412, 443 and 490 on selected stations of the ANT-XXVIII/5 cruise

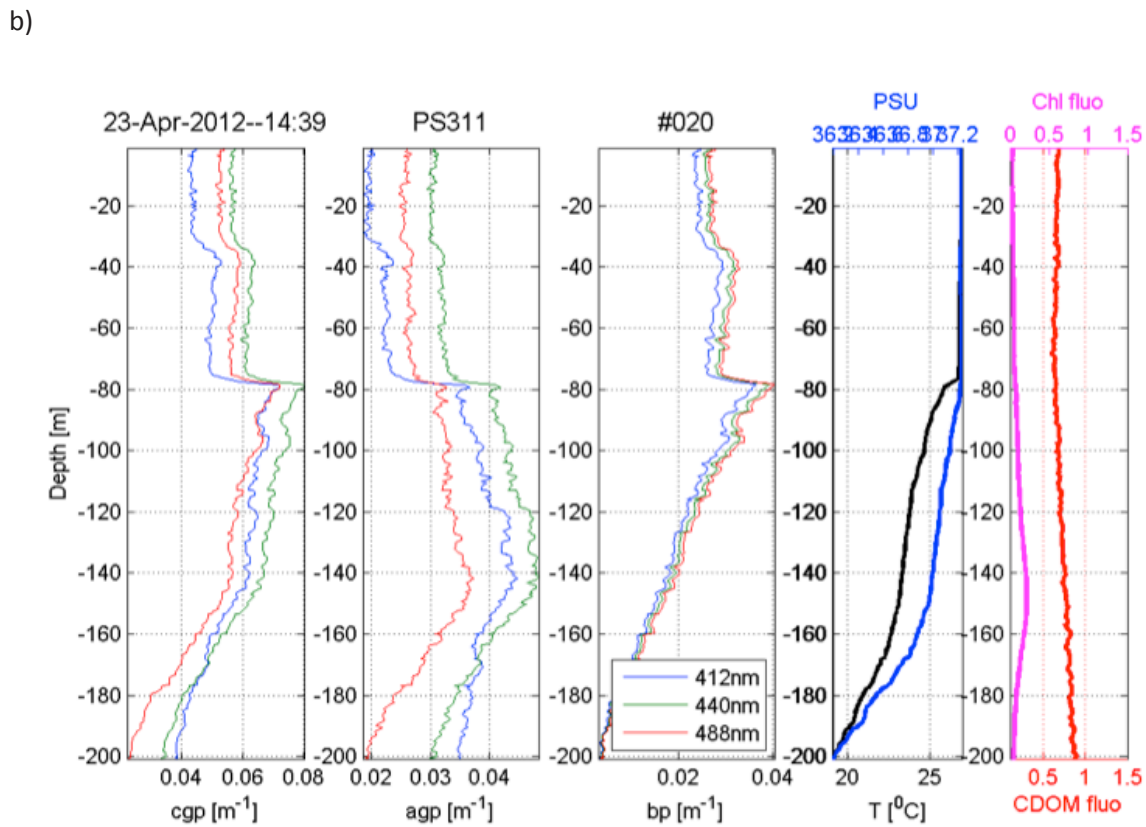
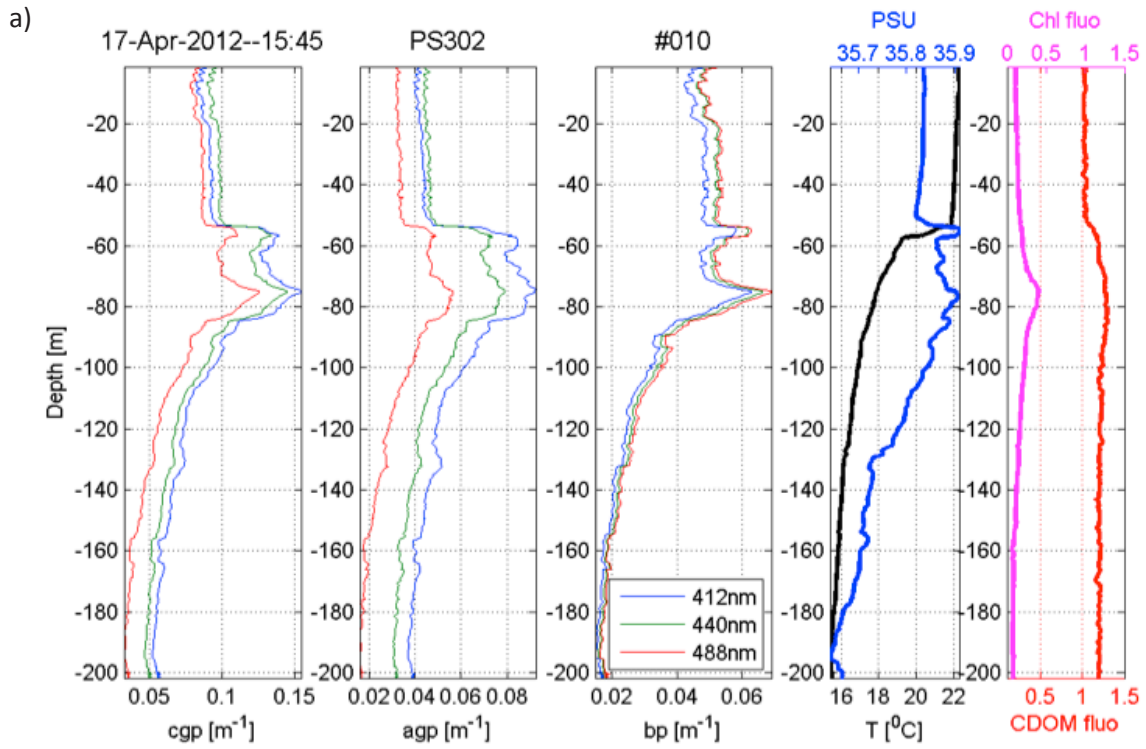
Data presented on four graphs of Fig. 3.1 showed the vertical profiles of downward irradiance recorded in different water masses. The downwelling irradiance at shortest waveband - 305 nm, diminishes first, and the solar radiation at visible part of the spectrum propagates deeper into water column. On all of them, you can clearly see that shapes and penetration depths of each spectral band varies significantly. The UV irradiance $E_d(305)$ penetrates in most cases down to 35-40 m in the open ocean oligotrophic waters (e.g. stations on 17 April, 2012 and 8 May, 2012). The strongest attenuation $E_d(305)$ was observed in the Bay of Biscay, which represents continental shelf water mass; the $E_d(305)$ disappeared already at 18 m depth. The optically clearest waters along this cruise, we found on 23 of April in tropical Southern Atlantic. The $E_d(305)$ penetrated down almost 60 m into water column. Solar irradiance in visible spectral bands were attenuated very weakly and at the depth of 120 values of $E_d(\lambda)$ in 412, 443, and 490 nm spectral

bands still had values around 10 Wm^{-2} . Such small decrease suggests that light in that particular water mass in visible spectral bands may penetrate much deeper than 200 m. Apart from differences in light attenuation in different spectral bands at given place and time there are noticeable differences in the rate of attenuation visible on the graphs as the change of the slope in the vertical profile of $E_d(\lambda)$. For example, there is noticeable change in attenuation rate of $E_d(305)$, $E_d(320)$, $E_d(3340)$ and $E_d(380)$ in vertical profiles recorded on 17 and 23 April, 2012 and in visible spectral bands $E_d(412)$, $E_d(443)$ and $E_d(490)$ in vertical profiles recorded on 8 and 11 of May 2012. The change in attenuation rate of spectral downwelling irradiance has been effected by changes in vertical distribution of optically significant water constituents that change values and spectral properties of inherent optical properties. Downwelling irradiances presented on Fig 3.1 depend on solar incident irradiance transmitted through the atmosphere to the water surface, processes of light transmission through the water surface (wind and wave conditions) and the inherent optical water properties.

The influence of the latter can be assessed by measurements of light attenuation, absorption and scattering coefficients and fluorescence of CDOM and chlorophyll. Vertical distribution of those parameters are presented on Fig. 3.2 a,b,c,d, for the same stations as selected for Fig. 3.1. Additionally the temperature and salinity distributions are presented, as the vertical structure of water optical properties reflect, if present, distribution of suspended material over the depth, which in turn follows the density structure of the water column. Higher values of attenuation, absorption and scattering coefficients correspond to the water of lower transparency. Corresponding panels showing vertical distribution of particles volume concentration are presented of Fig. 3.3.

The common feature on Fig. 3.1 is changes of the slope of the vertical distributions of $E_d(\lambda)$ at certain depths. This is result of changes in water transparency due to varying presence of optically significant water constituents. On the 17 of April the broad maximum of light attenuation at depths below 55 was observed, as a result of accumulation of particles at T and S gradient and phytoplankton presence. This resulted in the loss of radiance $E_d(\lambda)$ within and below the layers, seen as the change of the slope. Similar effect can be observed on 23 of April and 8 of May. Different pattern of TS and optical water stratification on the station of 11th of May (low transparency water on the surface layer, higher in deeper layers) led to higher slope of $E_d(\lambda)$ in more transparent water layer. Distribution of light scattering coefficient ($b_p(\lambda)$) along the water column is in line with particles volume concentrations presented on Fig. 3.3. The thorough examination of optical water spectral properties with relation to CDOM concentration measured by water samples will be performed after final post cruise data processing.

Information of optical stratification of inherent water optical properties will allow for the estimation the depth of 0.1 % $E_d(\lambda)$, if the profiling has ended before reaching this level. This is especially the case of the station of 23 April, where the clearest waters were observed during this expedition. It is expected the 0.1 % of $E_d(\lambda)$ depth would reach 200 m and below.



3. Sources and transformation of CDOM in Atlantic Ocean

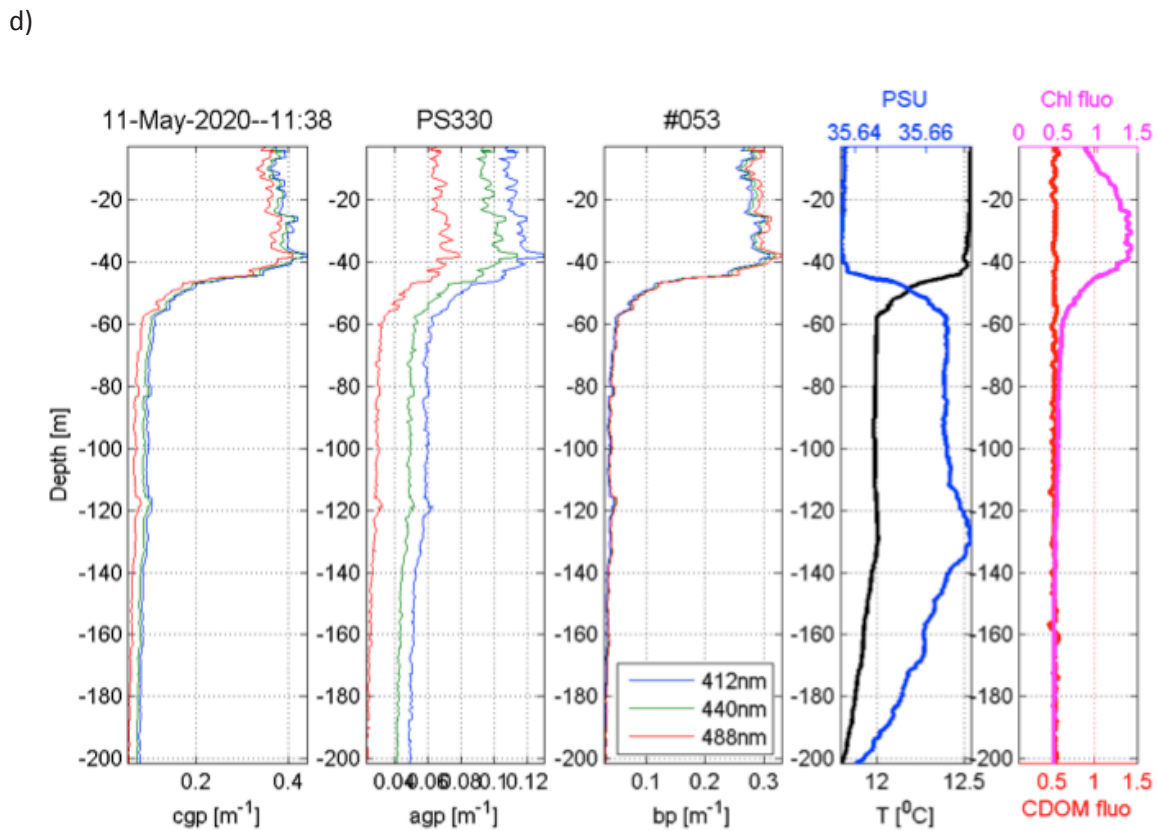
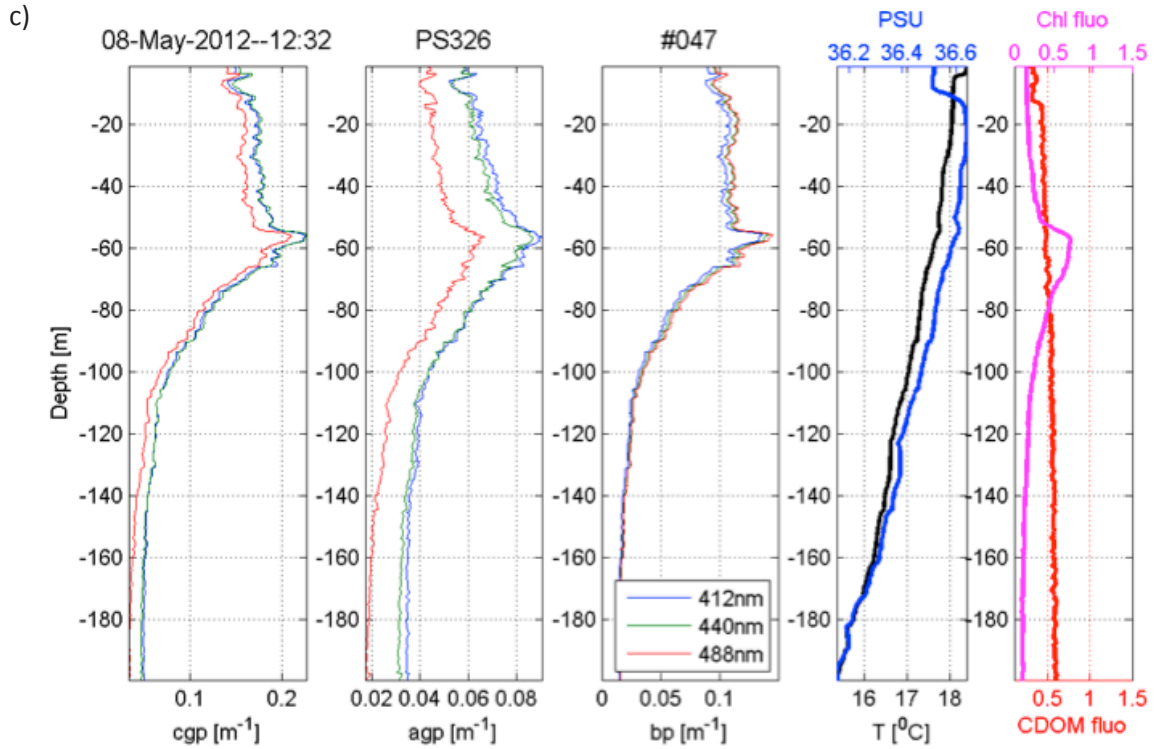


Fig. 3.2: Distribution of light attenuation by (cpg), absorption (agp) coefficients by particulate and dissolved materials, scattering coefficient by particles (bp) for 412, 440 and 488 nm wavelengths, temperature, salinity and fluorescence by CDOM and chlorophyll (in Volts, for range 0-5V) on selected stations of the ANT-XXVIII/5 cruise

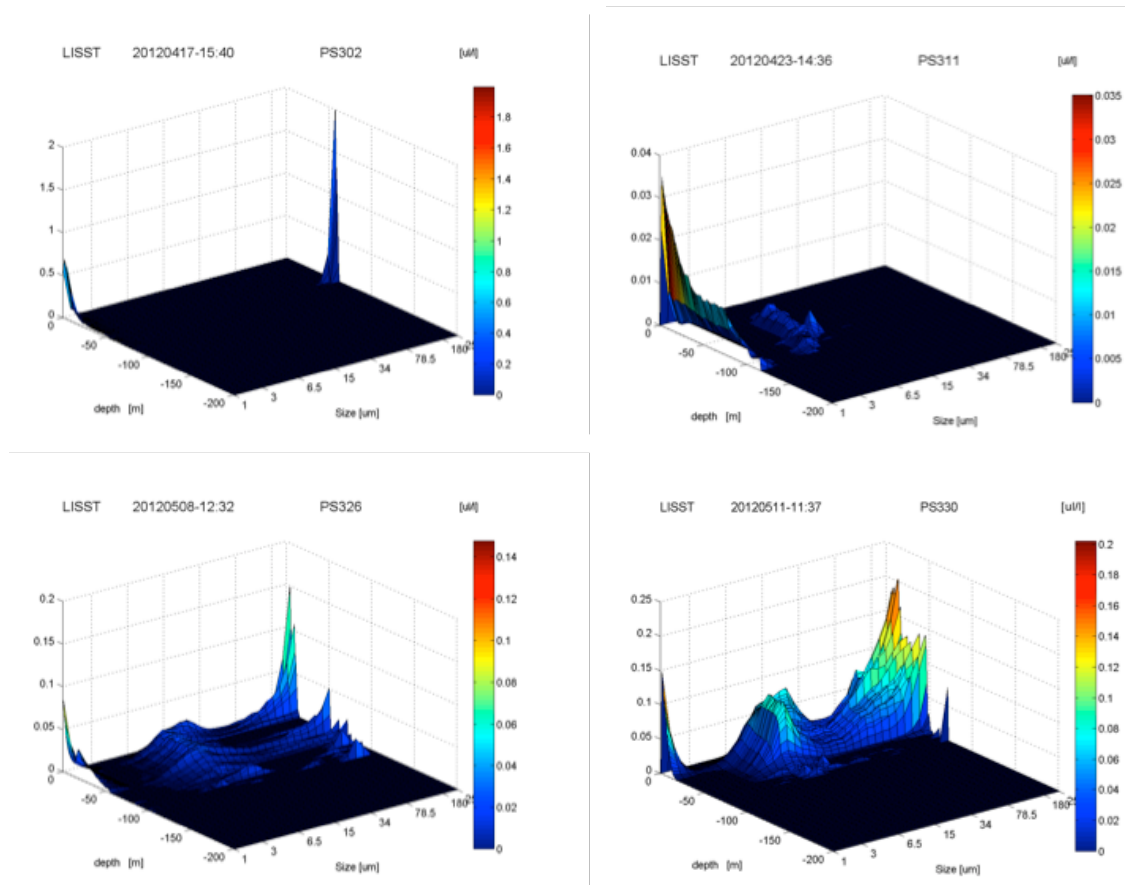


Fig. 3.3: Vertical distribution of volume particle concentrations on selected stations of the ANT-XXVIII/5 cruise. Size distribution for 32 size classes in range of 1.2 to 250 μm , logarithmic scale. The maxima of concentration in the area of surface water and the smaller size (0 m, 1 μm) are the artifacts of external incident light. Note the different scales of the concentration on each of the panel.

Data management

Almost all sample processing and data post processing will be carried out in the home laboratory at IOPAS. It usually takes one to three years depending on the parameter as well as analysing methods such as chemical measurements. As soon as the data sets are available they can be used by other cruise participants after request. When the data will be published they will be submitted to PANGAEA and are open for external use.

4. AUTONOMOUS MEASUREMENT PLATFORMS FOR ENERGY AND MATERIAL EXCHANGE BETWEEN OCEAN AND ATMOSPHERE (OCEANET)

Marlen Brückner¹, Karl Bumke³,¹IFT
Andreas Macke¹(not on board),²LIM
Michael Schäfer², Maik Merkel¹,³ GEOMAR
Denise Assmann¹, Susanne Fuchs¹,⁴ MPI
Susan Hartmann¹, Friederike Höpner¹,
Shan Huang¹, Michael Leistert¹,
Seethala Chellappan⁴,
Stefan Kinne⁴ (not on board)

OCEANET-Atmosphere

Objectives

Radiation, energy budget & microwave remote sensing

The net radiation budget at the surface is an important regulator in the climate system of the earth. It is mainly influenced by the complex spatial distribution of temperature and liquid water content in the atmosphere. The complex three-dimensional (3D) microphysical structure of clouds causes systematic errors in active and passive remote sensing of clouds, if the cloud variability is not resolved in radiative transfer models (RTM). Consequently, the retrieved cloud radiative properties and the cloud radiative energy budget might be biased.

With the Atlantic transfers of *Polarstern* it is possible to perform simultaneously observations under different atmospheric conditions in both hemispheres. The radiation budget and the cloud properties were observed in high temporal and even through the motion of the ship in high spatial resolution which provides realistic cloud-radiation interactions for use in remote sensing and climate models. Within the scope of the WGL-Project OCEANET the already existing broadband radiation measurements on *Polarstern* has been extended to spectral solar radiation measurements performing with a ship-based COmpact RAdiation measurement System (CORAS). CORAS simultaneously measures spectral resolved downward radiances and irradiances. Due to the spectral resolution of the spectrometers different contributions from different atmospheric gases and water vapour absorbing regions to the radiative quantities can be identified.

The Microwave Radiometer HATPRO provides continuously vertical profiles of humidity and temperature as well as time series for liquid water path (LWP) and cloud base high over the ocean. In combination with the variability of the downward radiative quantities these time series makes it possible to observe small scale atmospheric structures and cloud inhomogeneities.

Another goal of OCEANET is to estimate the energy budget at the air sea interface by measurements of all energy fluxes.

Work at sea

The OCEANET-Container was located on the helicopter deck on *Polarstern* (see Fig. 4.1). The measurements were performed underway and continuously. The following individual instruments were combined in the container:



Fig. 4.1: OCEANET-Container on the helicopter deck of Polarstern during ANT-XXVIII/5 (photo: M. Brückner)

OCEANET (Atmosphere)

For the broadband radiation measurements an upward looking Kipp&Zonen pyrgeometer CG 4 and pyranometer CM 21 supported from IFM-GEOMAR were used on this cruise.

A full sky imager with a camera system manufactured at IFM-GEOMAR was installed to obtain every 15 seconds whole sky images from the current atmospheric situation. This provides detailed information about the existing cloud coverage as well as the cloud type with a high temporal resolution.

The spectral radiations measurements of downward irradiance and radiance were obtained from CORAS. The optical inlets were installed at the top of the container (see Fig. 4.2). The measured radiation was transported to a spectrometer box in the container by optical fibers. The spectrometer splits up the radiation according to the wavelengths. The spectral range from CORAS is 350 - 2,000 nm. Under good weather conditions, CORAS was calibrated each day with a small Ulbricht-integrating sphere. It creates diffuse radiation from a directionally orientated radiation. To obtain the background noise in the data also a dark calibration was performed.

The multichannel microwave radiometer HATPRO was calibrated in Punta Arenas with liquid nitrogen. It performs continuously observations of atmospheric humidity and temperature profiles as well as integrated water vapour (IWP) and liquid water path (LWP).

Standard meteorology devices for obtaining the position of *Polarstern*,

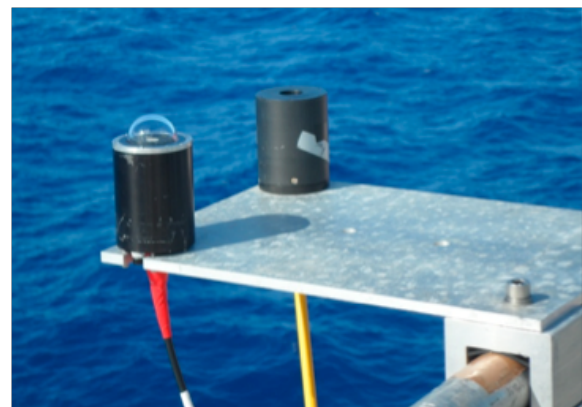


Fig. 4.2: Optical inlets from CORAS for spectral radiance (right) and irradiance (left) during ANT-XXVIII/5 (photo: M. Brückner)

speed and course over ground, temperature and humidity as well as pressure in sensor high and sea level were located on the container.

Measurements were completed by a turbulence measurement system mounted on the crew's nest, which enables together with radiation flux measurements to derive the energy budget at the air sea interface.

Preliminary results

Fig 4.3 shows the time series of downward spectral radiance and irradiance in the visible range (VIS) at pixel 500 (600 nm) for April 24, 2012. On this day there were only a few shallow cumulus clouds present which can be identified by the enhancement of radiance or irradiance. The enhancement results from the diffuse contribution of cloud edge scattering.

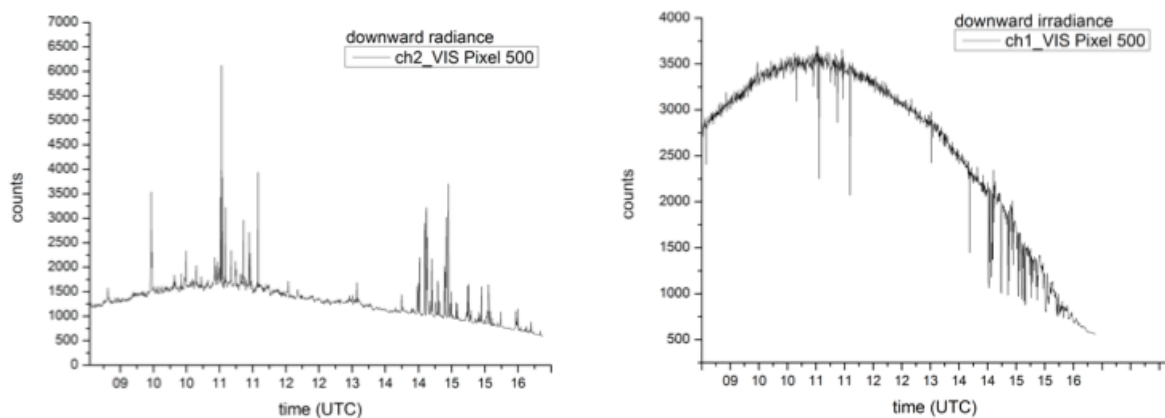


Fig. 4.3: Time series of downward radiance (left) and irradiance (right) for VIS at pixel 500 obtained from a measurement on *Polarstern* on April 24, 2012 (preliminary and uncorrected data)

The scientific goal of this part of the project is to compare the observation on *Polarstern* with different model calculations of the radiative quantities. With the aid of observed and modeled spectral transmitted radiance cloud properties such as cloud optical thickness (t) and effective radius (r_{eff}) were retrieved. The vertical cloud structure is obtained from the microwave radiometer measurements. The all sky camera provides information on the horizontal cloud variability. To quantify 3D cloud effects on the cloud transmissivity 3D Monte-Carlo radiative transfer simulations will be used. The simulated cloud transmissivity will be compared to simulations with a plan parallel RTM and the measurements of CORAS. Furthermore, cloud optical thickness and effective radius, will be retrieved by using both 3D Monte-Carlo and plan parallel radiative transfer simulations. Differences in the retrieved cloud properties will be systematically classified by cloud fraction and cloud vertical inhomogeneities derived from all sky camera and microwave radiometer.

Data management

The data processing will be carried out in the IfT and LIM, respectively. Some of the instruments will be calibrated in the home laboratory to determine the calibration parameters for correct data sets. This will properly takes several months. After post processing the complete data sets are available for other cruise participants after request.

5. CHEMICAL, PHYSICAL AND OPTICAL CHARACTERIZATION OF MARINE AEROSOLS

Maik Merkel¹, Denise Assmann¹, Susanne Fuchs¹, Susan Hartmann¹, Friederike Höpner¹, Shan Huang¹, Michael Leistert¹, Andreas Macke¹, not on board
Seethala Chellappan², Stefan Kinne²

¹Ift
²MPI

Objectives

The exchange of gases and aerosols between ocean and atmosphere has received considerable and intensive attention, but it is not well understood currently. Aerosol particles play an important role in the global climate change because of their effects on the radiation budget. This is particularly true for aerosols from marine environments. For this reason, the measurements on board *Polarstern* are to 1) better understand the formation mechanism of secondary fraction in marine aerosol particles, 2) investigate the interaction between sub-micron marine aerosols and water vapour under sub- and super-saturated as well as undercooling conditions, and 3) characterize the optical properties of marine aerosols.

Work at sea

To achieve the foregoing objectives, the physical laboratory container of IfT equipped with a number of scientific instruments was operated by seven scientists during the ANT-XXVIII/5 leg from Punta Arenas to Bremerhaven.

The chemical composition of marine aerosols was measured using both on-line and off-line systems. The Aerodyne High-Resolution Time-of-Flight Aerosol Mass Spectrometer (HR-ToF-AMS) provides quantitative measurements of the size resolved non refractory chemical composition of the submicron ambient aerosol at a typical time resolution of two minutes. Due to the 600°C surface temperature of the vapourizer, the AMS can only measure the non-refractory part of the particles. Soot, crustal material and sea-salt cannot be detected. Additionally to the AMS, PM₁ particles were sampled using a Digitel DHA-80 high volume sampler. Sampling was performed every day during 24h from midnight to midnight (UTC). Each PM₁ sample was collected on pre-backed quartz fibre filters. The filters will be transported to the laboratory to be analysed by state-of-the-art analytical instruments to determine the chemical composition of the collected particles.

Particle Number Size Distribution from 10 nm to 20 µm in diameter is measured by a Scanning Mobility Particle Sizer (SMPS) combined with an Aerodynamic Particle Sizer (APS). Both instruments have a time resolution of 5 minutes. The interaction between particles and water vapour under sub- and super-saturated conditions are respectively determined by Hygroscopicity Tandem Differential Mobility Analyser (HTDMA; relative humidity was 90 %) and Cloud Condensation Nuclei Counter (CCNC; with relative humidities from 100.07 to 100.7 %). Within these two instruments the hygroscopic growth and the activation behaviour of the

5. Chemical, physical and optical characterization of marine aerosols

particles can be determined. The activation behaviour is the probability of particles to form cloud droplets. Additionally, an Integrating Nephelometer and a Multi Angle Absorption Photometer (MAAP) as well as a Particle Soot Absorption Photometer (PSAP) were operated simultaneously to characterize the particle optical properties. They can measure the particle scattering and absorption coefficient and the black carbon concentration. Table 5.1 is showing a summary of scientific equipment to determine the properties of the marine aerosol on board *Polarstern*.

Tab. 5.1: Scientific instruments on board *Polarstern*

Instruments	Time Resolution	Data availability
Scanning Mobility Particle Sizer (SMPS)+ Aerodynamic Particle Sizer (APS)	5 min	11.04.-12.05.2012
Humidity Tandem Differential Mobility Analyser (H-TDMA)	5 min	13.04.-12.05.2012
Cloud Condensation Nuclei Counter (CCNc)	22 min	13.04.-12.05.2012
Multi Angle Absorption Photometer (MAAP)	1 min	12.04.-12.05.2012
Integrating Nephelometer	1 min	13.04.-12.05.2012
Particle Soot Absorption Photometer (PSAP)	1 min	12.04.-12.05.2012
High-resolution Time of Flight aerosol mass spectrum (HR-ToF-AMS)	2 min	13.04.-12.05.2012
Digitel filter sample	24 h	11.04.-12.05.2012
Water samples	Once daily	12.04.-10.05.2012

At the beginning of the cruise, the container was set up and all instruments were calibrated. The quality-control protocol was carried out to insure the high-quality data acquisition during the whole campaign.

For the most time of the campaign the wind was coming from ahead and brought ship contamination-free air. Especially when the ship stopped at the daily station time, an influence of contamination from the ship exhaust could be seen frequently. Beside this, the measurements were successful until 12 May, when the packing of the instruments started. A rough summary of data availability is given in the last column of Table 5.1.

In parallel to the chemical and physical characterization of the marine aerosol, water samples were taken to investigate the chemical composition of the ocean surface film once per day. These samples were collected around 500 m away from the ship by using a small boat. Each time, water samples were taken in 2 m depth and on water surface, respectively. In total, we took water samples at 26 stations.

The samples were separated and stored at -20°C. They will be analysed in the chemistry lab in Leipzig concerning their organic content.

A MICROTOPS Sun Photometer was used to take the aerosol measurements onboard *Polarstern*. This dataset is also a contribution to the well-known AERONET (NASA based) project. MICROTOPS measures Aerosol Optical Thickness (AOT) values at 380-440, 440-675, 675-870, 870-936 micron wavelengths based on the channel's signal, its extraterrestrial constant, atmospheric pressure (for Rayleigh scattering), time and location. The daily observations were taken at clear sky conditions, and also carefully when the Sun's disc is not obscured by clouds in case of partial clouds. No measurements were taken in presence of clouds/rain and also when the ship was on station. The observations were taken at 5 or 10 minute intervals. The datasets comprise of 3250 individual scans (roughly 25 – 30 individual measurements per day). On 17 days no measurements took place due to cloudiness. On two days we had Saharan dust, accordingly our observations clearly showed very high AOT values over there.

Preliminary (expected) results

Based on the on-line measurements and the off-line analyses, the size-dependent chemical and physical properties of near-surface marine aerosols and the chemical composition of ocean surface films will be obtained.

A detailed analysis on AMS data will provide chemical information of aerosol particles such as the ratio of oxygen to carbon, the relative abundance of hydrocarbon-like structures, and a variety of molecular fragments. Therefore, to some extent, we can gain insight into the formation mechanism of marine aerosols, especially organic fraction.

The hygroscopic growth and activation measurements can provide information about the particle mixing state, the growth factor, the critical diameter for the activation, and the cloud droplet number distribution of the aerosol particles. By combining the data to the chemical measurements a closure study will be performed.

The light extinction at ambient humidity can be predicted from *in-situ* measurements of dry and humidified particle number size distributions, light scattering and absorption coefficients, and size-resolved chemical composition. Optical properties of aerosol particles and *in-situ* physical and chemical measurements as well as columnar optical property measurements can be used to establish a connection between *in-situ* ground and columnar aerosol properties.

During the cruise ANT-XXVIII/5 the ambient aerosol originated mainly from marine sources. Fig. 5.1 shows the particle number size distribution as a function of time measured by the SMPS. As it can be seen on April 29 the air mass changed and the number concentration increased. One day later (April 30) the measurements were influenced by mineral dust particles originating from the Sahara. Especially for coarse mode particles the number concentration increased sharply.

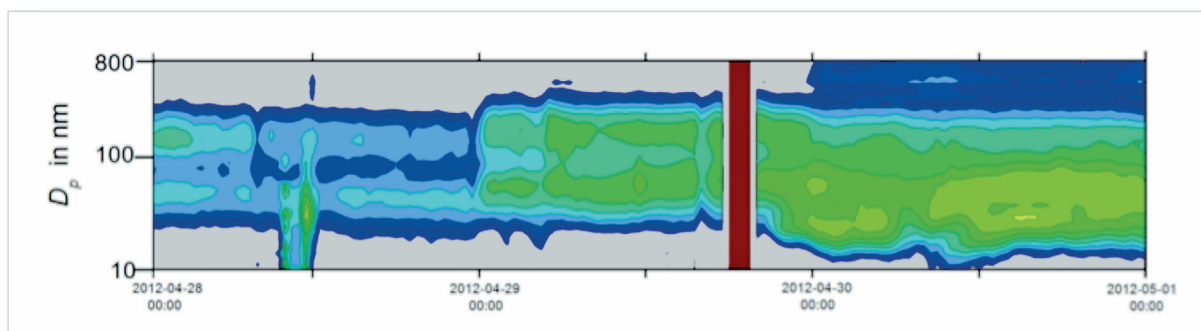


Fig. 5.1: Particle number size distribution measured by the SMPS for three days showing different aerosol particles and number concentrations

Fig. 5.2 is showing a first result of the chemical particle composition measured with the AMS. For April 29 an increase of sulphate, ammonium and organics was observed. Due to the upper limit of around 1 μm in particle diameter for the AMS measurements the dust event with coarse mode particles cannot be seen with this instrument. Sulphate and organic mass concentration remained on a higher level during this event than for the marine size distribution.

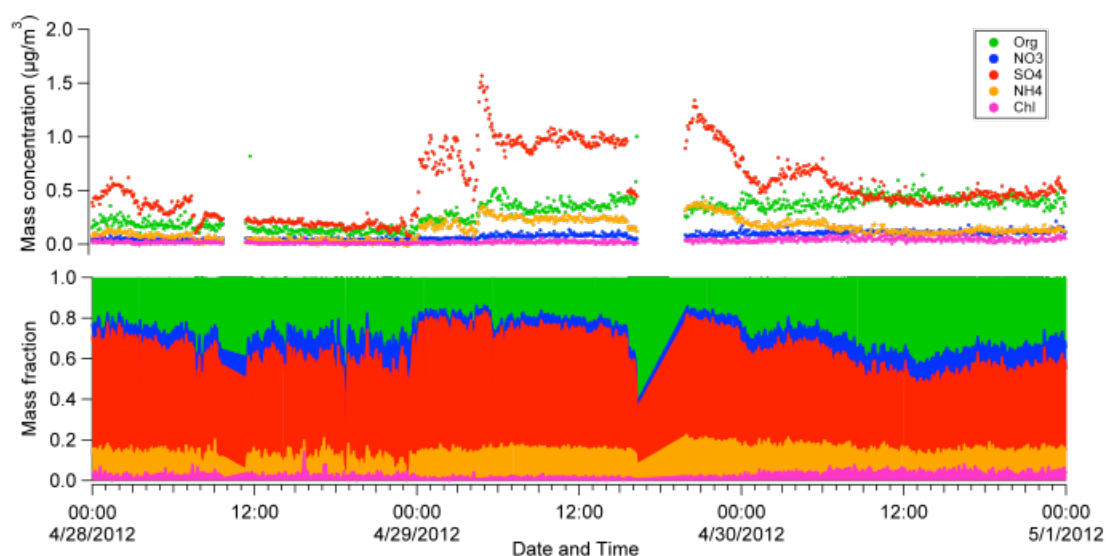


Fig. 5.2: Particle mass concentration and mass fraction for the chemical compounds organics (Org), nitrate (NO_3), sulphate (SO_4), ammonium (NH_4) and chloride (Chl)

The lower graph of Fig. 5.2 shows the mass fraction of the different chemical species. When the ship entered the dust plume the organic fraction increased while the sulphate fraction decreased slightly. But in total the mass fraction remains more or less the same for the given time period.

The left graph of Fig. 5.3 represents the absorption coefficient measured by the MAAP at a wavelength of 637 nm. Because of the time resolution of one minute and a noisier signal from the instrument, the displayed data are soothed by an average of five minutes. On the right the backscattering coefficient for three different wavelengths (blue 450 nm, green 550 nm and red 700 nm) can be seen.

For marine aerosols the absorption and the backscattering coefficients have lower values. Due to the properties of marine aerosol particles approximately 95 % of radiation will be scattered forward. When the dust event started on April 30 both coefficients increased due to the changed conditions in the atmosphere. Dust particles are absorbing more radiation than marine particles and due to the shape of them light is also scattered backwards.

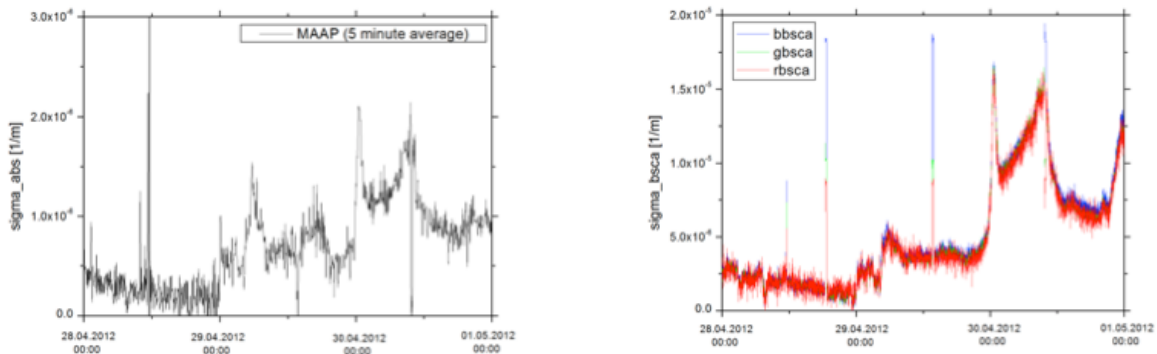


Fig. 5.3: Absorption and backscattering coefficient from MAAP and Integrating Nephelometer for the change from marine aerosols to dust aerosols

The growth factor for particles with a diameter of 100 nm is shown in Fig. 5.4. It correlates well with the mass fraction of sulphate and organics. A higher mass fraction of sulphate results in a higher value for the growth factor. For most organic compounds the growth factor decreases with higher mass fraction.

The critical diameter D_{crit} is a measure for the ability of an aerosol particle to act as a Cloud Condensation Nucleus (CCN). The lower the value of D_{crit} the lower is the super-saturation needed for droplet activation. D_{crit} strongly depends on particle size and the chemical composition of the ambient aerosol particles.

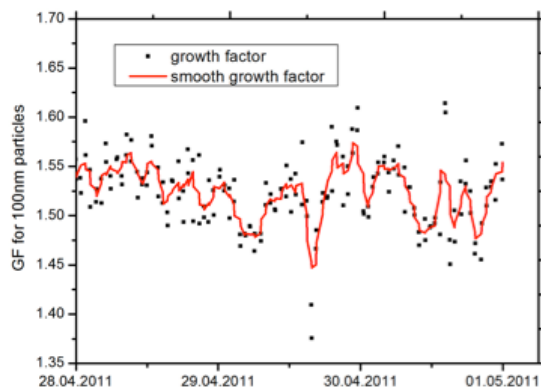


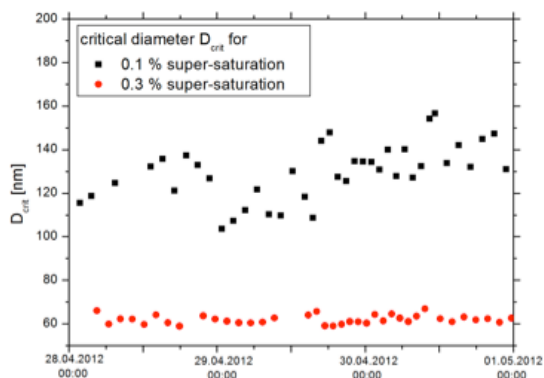
Fig. 5.4: Growth factor for 100 nm particles measured with the HTDMA for the time period April 28 to May 1

Exemplarily, preliminary data of ambient measurements for a time series of D_{crit} are shown in Fig. 5.5 for 0.1 and 0.3 % super-saturation. Considering 0.3 % super-saturation D_{crit} is almost constant at 60 nm within the time period 28.04.-30.04.2012. This suggests that all the aerosol particles are already being activated to cloud droplets under these conditions.

In contrast, the measurements performed at 0.1 % super-saturation are more sensitive on changes aerosol particle composition. On 28 April 2012, the measurements were partly influenced by the ship exhaust. D_{crit} values decreased beginning on 29 April and increased again to a higher level of about 140 nm in

average. This finding might be related to a Saharan dust event, which means that mineral dust from the Saharan desert was transported to the Atlantic Ocean. As a result the typical marine aerosol was mixed with Saharan dust. Thus, mineral dust is composed of species, most of them being insoluble, the measured aerosol particles are activated to cloud droplets at higher super-saturations than the aerosol particles containing more soluble species as for instance the typical marine aerosol particles.

Fig. 5.5: Critical diameter of aerosol particles for activation to cloud droplets for the time period April 28 to May 1



Data management

All data and sample processing will be carried out in the home laboratory at IfT. It will usually take around one to two years until the first results of water probes and filter measurements will be available. The online measurements of aerosol particles might need some months to insure the quality of the data set. As soon as the data are available they can be used by other cruise participants on request.

6. COMPOSITION AND ACTIVITY OF THE BACTERIOPLANKTON COMMUNITIES IN A SOUTH-NORTH TRANSECT OF THE ATLANTIC OCEAN WITH A SPECIAL EMPHASIS ON THE ROSEOBACTER CLADE AND DISSOLVED ORGANIC MATTER

Meinhard Simon¹, Sara Billerbeck¹, Alexander Gavrilov¹, Helge A. Giebel¹, Siri Rackebrand¹, Thomas Remke¹, Maren Stumm¹, Maren Seibt¹, René Ungermann¹, John Vollmers³, Irene Wagner-Döbler², Hui Wang², Matthias Wietz¹, Mascha Wurst¹

¹ ICBM

² HZI

³ Uni Gö

Objectives

We aim at a comprehensive assessment of bacterioplankton communities from subantarctic south Atlantic to temperate north Atlantic water masses with a special emphasis on the *Roseobacter* clade and its major bacterioplankton subclusters. This project is part of a key work package of the Transregional Collaborative Research Center *Ecology, Physiology and Molecular Biology of the Roseobacter clade: Towards a Systems Biology Understanding of a Globally Important Clade of Marine Bacteria* (TRR 51).

Tab. 6.1: List of parameters studied for assessing bacterioplankton communities during cruise ANT XXVIII/5

Parameter	20 m	40 m	60 m	100 m	200 m	500 m	≥1000 m
POC	+	+	+	+	+		
Chlorophyll a	+	+	+	+	+		
Phytoplankton	+	+	+	+			
Inorganic nutrients	+	+	+	+	+	+	+
Bacterial abundance	+	+	+	+	+	+	+
Bacterial production	+	+	+	+	+	+	+
Glucose turnover rate	+	+	+	+	+	+	+
Amino acid turnover rate	+	+	+	+	+		
FISH	+	+	+	+	+		
Microautoradiography-FISH	+		+	+			

6. Bacterioplankton communities in a south-north transect of the Atlantic Ocean

Parameter	20 m	40 m	60 m	100 m	200 m	500 m	≥1000 m
Aerobic anoxygenic bacteria	+	+	+	+	+		
DGGE	+	+	+	+	+	+	+
Pyrosequencing of 16S rRNA gene	+	+	+	+	+	+	+
Metagenomics	+		+				+
Metatranscriptomics	+	+	+	+	+	+	+
Dissolved amino acids	+	+	+	+	+		
Dissolved carbohydrates	+	+	+	+	+		
DOC	+	+	+	+	+	+	+
DOM	+	+	+	+	+	+	+
Vitamins	+	+	+	+	+	+	+

The work includes investigations of the biogeography, growth and population dynamics, the genomic potential (metagenomics) and actively expressed genes (metatranscriptomics) and the impact on the decomposition of dissolved organic matter (DOM) and cycling by the bacterioplankton communities. Our investigations can only be done in a concerted action in which also the other members of the bacterioplankton communities are considered, as well as bulk parameters of the entire bacterioplankton communities and relevant biogeochemical parameters such as chlorophyll and the composition and concentration of DOM. Previous studies dealing with some of these aspects have been carried out before in the Atlantic Ocean (Mary et al., 2006, Zubkov et al., 2008, Schattenuhofer et al., 2009, and Gomez-Pereira et al., 2010). However, one particular group of marine bacteria and in particular the *Roseobacter* clade have not been investigated before in such great detail.

A list of investigated parameters is given in Table 6.1.

Tab. 6.2: List of stations and depths investigated for studies of the bacterioplankton and dissolved organic matter during cruise ANT XXVIII/5

Station	Date (2012)	Ship time	Latitude S/N	Longitude W	Depth (m)	Sampled Depths (m)
296	11.04.	14:20	51° 03.26' S	66° 27.75'	120	20-100
297	12.04.	14:15	47° 56.44' S	61° 55.21'	134	20-100
298	13.04.	13:00	45° 05.62' S	58° 09.79'	2954	20-200, 500, 1000, 2000
300	15.04.	14:00	39° 47.91' S	50° 34.74'	5376	20-200
302	17.04.	13:00	34° 14.28' S	42° 57.90'	4566	20-200
304	18.04.	16:30	30° 59.94' S	38° 59.69'	4161	20-200, 500, 1000, 2500, 4000
307	20.04.	13:30	24° 45.27' S	38° 01.04'	3897	20-200
308	21.04.	15:30	21° 13.64' S	35° 23.96'	4328	20-200
310	22.04.	13:30	18° 38.73' S	33° 43.81'	4340	20-200, 500, 1000, 2500, 4000

Station	Date (2012)	Ship time	Latitude S/N	Longitude W	Depth (m)	Sampled Depths (m)
312	24.04.	13:30	11° 53.91' S	29° 45.07'	5498	20-200
313	25.04.	13:30	08° 12.66' S	27° 59.44'	5611	20-200
314	26.04.	10:30	05° 05.81' S	26° 38.39'	5668	20-200 500, 1000, 2000
315	27.04.	13:30	01° 29.27' S	25° 19.25'	4945	20-200
317	29.04.	13:30	06° 03.54' N	23° 28.84'	4255	20-200 500, 1000, 2500, 4000
318	30.04.	13:30	09° 34.36' N	22° 46.32'	4878	20-200
319	01.05.	13:30	12° 35.36' N	22° 11.74'	4854	20-200 500, 1000, 2500, 4000
320	02.05.	14:30	16° 54.27' N	21° 34.10'	3644	20-200
321	03.05.	14:15	20° 42.28' N	21° 10.25'	4092	20-200
322	04.05.	13:30	24° 23.75' N	19° 52,07'	3043	20-200 400, 900
323	05.05.	13:50	26° 20.95' N	17° 18.77'	3615	20-200
324	07.05.	13:30	33° 23.92' N	13° 32.08'	4419	20-200
326	08.05.	12:00	35° 14.25' N	12° 53.63'	2778	20-200 600, 1100
328	09.05.	11:30	38° 44.74' N	12° 36.52'	4564	20-200 500, 1000
329	10.05.	13:30	43° 02.58' N	10° 56.15'	2707	20-200
330	11.05.	13:30	47° 02.66' N	08° 05.44'	4252	20-200

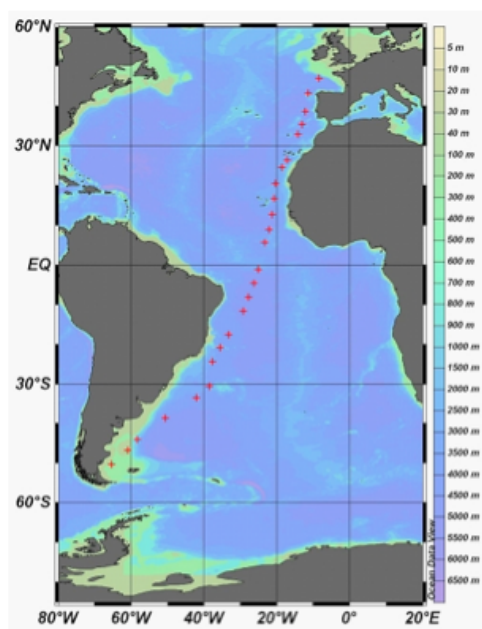


Fig. 6.1: Map with stations where samples for this study were collected during cruise ANT- XXVIII/5

Work at sea

Our main work on shipboard was the collection and processing of water samples from depths between 20 and 4,000 m between the subantarctic waters on the Patagonian Shelf and the north-western Atlantic. Samples were collected with Niskin bottles mounted on a CTD rosette from the mixed layer, the mesopelagic and bathypelagic zones. Our sampling scheme included fixed depths between 20 and 200 m and at deep stations also at 500 and 1,000 m. Below,

sampling depths were identified according to water masses and the temperature and salinity profile. In total 25 stations including 9 deep stations were visited. For exact locations and further details see Table 6.2 and Fig. 6.1.

6. Bacterioplankton communities in a south-north transect of the Atlantic Ocean

At all stations and in most cases, samples were filtered onto membrane filters of various type and size, frozen at -20 or -80 °C and further processing will be done in the home labs. Samples for phytoplankton and nutrient analyses were fixed with Lugol's solution and will also be analysed in the home lab. Samples for the analyses of dissolved amino acids, carbohydrates, vitamins, DOC and DOM were prefiltered and frozen or acidified (DOC) and will also be analysed later upon arrival in the home labs. Samples for bacterial abundance, production and turnover of dissolved free amino acids and glucose were analysed on shipboard. Bacterial abundance was assessed by flow cytometry and bacterial production and substrate turnover by radiotracer techniques and applying ¹⁴C-leucine, ³H-leucine, -glucose and -amino acids. For details on the methods see Simon and Azam (1989) and Simon and Rosenstock (2007).

Preliminary results

Temperature and salinity indicate that we were in subantarctic water masses south of 42.5 °S, where we crossed the Subtropical Front (STF). The south Atlantic subtropical gyre ranged from the STF to the equatorial upwelling around 2-6°N (Fig. 6.2). Further north and coming closer to the eastern Atlantic with the Mauritanian upwelling and Canary Current temperature continuously decreased until we reached the final station at 47°N.

Integrated bacterial biomass production varied greatly over the entire transect

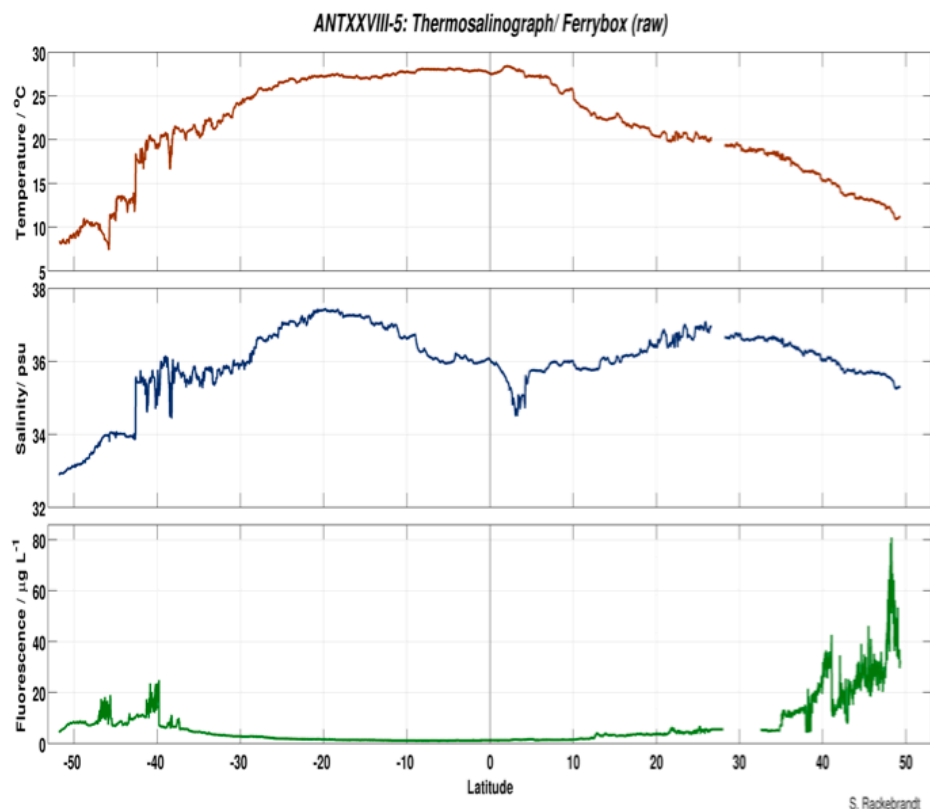


Fig. 6.2: Uncalibrated sea surface temperature, salinity and chlorophyll fluorescence between 52 °S and 49 °N in the Atlantic as measured by the ships's salinometer and ferry box

and did not show a clear-cut relationship to water masses or temperature. Lowest values occurred in the region south of 34 °S, at 25 and 2 °S and at 43 °N west of Galicia, NW Spain. Highest values occurred in the tropics, constraint by the latitudes 20° S and N. However, high rates were also recorded at 31 °S at the Vema Channel and at 39 °N west of Portugal (Fig. 6.3).

Bacterioplankton bulk generation times in the upper 100 m were substantially longer south of the subtropical front as compared to further north. South of this front they were at least 3 days and up to 10 days whereas further north they were in most cases shorter than 3 days with shorted generation times of less than 1.5 days at some stations in the tropics.

Turnover times of dissolved free amino acids in the upper 100 m were longer south of 5 °S and north of 28 °N than within this north tropical region. Whereas they were in most cases longer than 10 days in the southern and northern regions they were always shorter in the northern tropical region and often shorter than 4 days.

How these data relate to other parameters such as water temperature, mixed layer depth, concentrations of chlorophyll *a*, DOC, dissolved amino acids and carbohydrates. The most interesting question is whether and how these data will be reflected in the composition and metabolic activities of the bacterioplankton communities at these stations. Our analyses hopefully will shed light on this issue.

These results and those of all other parameters for which samples were collected, however, will become available only after processing of the samples in the home labs after several months to years.

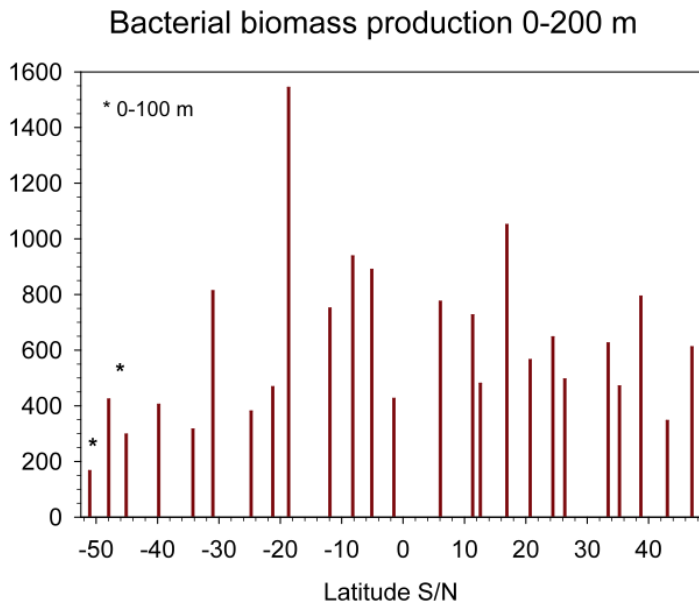


Fig. 6.3: Bacterial biomass production integrated from 0 to 200 m at all stations visited during cruise ANT-XXVIII/5

Data management

All finally processed data will be stored on a server at ICBM and of TRR 51 and will be available on request if not otherwise mentioned. Data on the pyrosequencing and metagenomics and meta-transcriptomics will be processed and stored on a server of the Göttingen Genomics lab at the University of Göttingen and at HZI. The final data of the metagenomics and metatranscriptomics and on sequenced genes will be made publicly available via GenBank and NCBI. Most of the data will be published in international peer-reviewed journals.

7. HIGHER TROPHIC LEVELS: DISTRIBUTION OF MARINE MAMMALS AND SEABIRDS AT SEA

René-Marie Lafontaine^{1,2}, Roseline C, ¹PoIE
Beudels^{1,2}, Oria Jamar de Bolsée^{1,2} ²RBINS
Claude Joiris¹ (not on board)

Objectives

In the framework of PoIE's long-term studies of the at-sea distribution of seabirds and marine mammals, special attention is paid, during cruise leg ANT-XXVIII/5, to less studied open Oceanic zones such as the Argentine and Brazilian basins.

We are particularly interested in the mechanisms underpinning this distribution: water masses and ocean floor structures such as continental slopes which influence the localization of fronts, upwelling, etc. We also aim at determining the correlation between observed distributions of higher vertebrates with oceanic bio-geographical provinces defined on the basis of phyto- and zoo-plankton (i.e. Longhurst, 2007). Of special interest are the complementary studies of the main prey of seabirds and cetaceans: zooplankton and krill, nekton, and small fish (Joiris & Falck, 2010).

Work at sea

Continuous transect counts are carried out from the bridge of Polarstern, from sunrise to sunset, divided in periods of 30 minutes. Every individual detected with naked eyes is counted and optics (binoculars x10 and telescopes x30) were used to confirm the species identification. Field guides (Carwardine, 1995; Shirihai, 2006; Shirihai, 2008; Onley & Scofield, 2007) were used to confirm identification when necessary. Coordinates were recorded at the beginning of each counting period, together with potential variables such as depth, water temperature (taken as proxies for more direct parameters like prey availability). Visibility was also recorded as a co-variable, as it can bias the total estimates.

Preliminary (expected) results

We conducted 655 counts so far (13 May) representing 327,5 hours of counting, with a total of 6625 birds of 55 marine species (e.g. Fig. 7.1), with a mean number of 10.1 birds per counting period. As an example some observations are given in Table 7.1.

Important differences were noted between the very rich South West Atlantic Shelf (FKLD or Patagonian Shelf) or rich North-Eastern Atlantic Shelf and the near-desert South Atlantic Gyre Province (SATL).

Through the South West Atlantic shelf (FKLD) and the South sub-tropical convergence (SSTC), the number of birds went from around 50 per counting periods, with a mean of 80 birds along the shelf, down to a mean of 32,3 in the convergence. As we entered the South Atlantic Gyre Province (SATL), numbers went down drastically to 2 to 5 per counting period, to reach the desert-like Western tropical

7. Higher trophic levels: distribution of marine mammals and seabirds at sea

Atlantic Province (WTRA) and North Atlantic Tropical Gyre (NATR) with near 0 (0.05) per counting period. Number of observations increased to 3,5 birds per counting period as we approached the Cape Verde archipelago and the Canary's cold current/upwelling, in the North Atlantic sub-tropical gyre. In the North Atlantic Drift Province (NADR) and the Northeast Atlantic Shelves (NECS) areas the mean number per counting period increased again to 9,9 birds. One very interesting counting period was on the 8 of May when unusually good numbers of *White-faced Storm-Petrel* (30) and *Madeiran Storm-Petrel* (15) were observed just over a sea mount.

As for the marine mammals, fourteen different species were observed and identified. This include *Sperm whales*, *Humpback whales*, *Bryde's whales*, *Sei whales*, *Fin whales*, *Short-finned Pilot whales*, a *Ziphiidae* (possibly *Blainville's Beaked whale*), as well as 5 species of *dolphins* and *porpoises* including the *Atlantic Spotted dolphin*, *Peale's dolphin*, the *Short-snouted Spinner dolphin*, *Dusky dolphin* and the *Harbour porpoise*. *Austral fur seals* were also spotted near the ship on the Patagonian shelf.

Further research will reveal if there are clear correlations with oceanographic and biological parameters, such as water quality parameters, seafloor topography, plankton blooms or krill, fish concentrations and total biological activity in the form of chlorophyll levels. This knowledge can then be used for the mapping of vulnerable areas.

Comparing our raw data with the data collected by Goffart et al. during ANT-XXVIII/1 in November 2011 on the Bremerhaven-Cape Town transect show that general geographical distribution of birds density is similar, with richest areas in the temperate shelf zones and very poor areas in the tropical Atlantic gyres. As for species' distribution, results seem to be rather different. This is probably due in large part to the different seasons and partly to the routes followed.



Fig. 7.1: *Cory's Shearwater Calonectris diomedea* on Atlantic Ocean near Canaries Island. Photo: Philippe Goffart, POE

Data management

Treatment of all the data will be done when all the data of the present cruise and the ANT XVIII-1 cruise, from Bremerhaven to Cape Town, will be integrated and verified. This analysis will try to find correlations between seabirds (and sea mammals) densities and environmental variables.

It is too early to discuss the interest of a regular monitoring renewed annually from the *Polarstern* along the Atlantic, as the analysis of all the data of this first return journey trial has to be finalized. However, it already clearly appears as an interesting opportunity which could be further explored.

All seabird and mammal data are available in the PoE data set (joiriscr@gmail.com).

Tab. 7.1: Example of observation statistics

DATE		04.11.2012	04.12.2012	13.04.2012
COORDINATES FIRST		51°44'15" S - 67°06'50" W	48°44'45" S - 63°03'59" W	45°41'58" S - 58°59'26" W
COORDINATES LAST		50°30'57" S - 65°39'05" W	47°29'48" S - 61°19'40" W	44°51'53" S - 57°47'53" W
WATER TEMPERATURE (Celsius)		8,3	10,3	10,8
DEPTH (meters)		100	130	1697-3420
COMMENT				Very foggy all day long
n (number of counting periods)				
		655	16	19
				14
Sea Birds	Oiseaux marins	Aves		
Magellanic Penguin	Manchot de Magellan	<i>Spheniscus magellanicus</i>		13
Rockhopper Penguin	Gorfou sauteur	<i>Eudyptes chrysocome</i>	2	1
Penguin sp	Manchot sp.	<i>Spheniscidae sp</i>		1
Wandering Albatross	Albatros hurleur	<i>Diomedea exulans sl</i>	2	8
Northern Royal Albatross	Albatros de Sanford	<i>Diomedea sanfordi</i>	4	1
Southern Royal Albatross	Albatros royal	<i>Diomedea epomophora</i>		12
Royal Albatross sp	Albatros royal sl	<i>Diomedea epomophora sl</i>		5
Large Alabtross sp	Grand albatros	<i>Diomedea sp</i>		
Black-browed Albatross	Albatros à sourcil noir	<i>Thalassarche melanophris</i>	145	77
Atlantic Yellow-nosed Albatross	Albatros à nez jaune	<i>Thalassarche chlororhynchus</i>		
Albatross sp	Albatros sp	<i>Thalassarche sp</i>		42
Northern Giant Petrel	Pétrel de Hall	<i>Macronectes halli</i>	3	
Southern Giant Petrel	Pétrel géant	<i>Macronectes giganteus</i>	4	7
Giant Petrel sp	Pétrel géant sl	<i>Macronectes sp</i>	13	11
Long-tailed Skua	Labbe à longue queue	<i>Stercorarius longicaudus</i>		3

8. MEASUREMENT OF THE OXYGEN ISOTOPE ANOMALY (^{17}O -EXCESS) OF OZONE FROM 53°S TO 53°N IN THE ATLANTIC MARINE BOUNDARY LAYER

William C. Vicars¹
Not on board: Samuel Morin²,
Joël Savarino¹

¹LGGE/CNRS,
²Météo-France/CNRS

Objectives

Recently, there has been considerable interest in using the oxygen isotopic composition of various atmospheric compounds as an interpretive tool to quantify and constrain the rates of atmospheric processes. The unique and distinctive oxygen isotope anomaly, or ^{17}O -excess ($\Delta^{17}\text{O}$), of ozone has proved to be a particularly useful isotopic fingerprint in such studies. The $\Delta^{17}\text{O}$ signature of ozone is transferred through oxidation reactions to other oxygen bearing compounds such that the $\Delta^{17}\text{O}$ values of atmospheric species act as fingerprints for the influence of ozone in their chemical formation pathways. This isotopic fingerprint cannot be removed or altered via subsequent fractionation processes and is thus conserved during atmospheric transport and processing. This isotope transfer provides a unique approach for tracing chemical oxidation pathways in the atmosphere and has yielded valuable insight into the modern atmospheric cycling of nitrate, sulfate, CO_2 , and N_2O (Morin et al., 2008; Röckmann et al., 2001; Savarino et al., 2003). Furthermore, variations in the $\Delta^{17}\text{O}$ values of atmospheric species contained in ice cores may serve as useful proxies for paleofig-oxidation chemistry, providing a means for the extension of atmospheric interpretations into the past.

Although there have been numerous tropospheric studies which report $\Delta^{17}\text{O}$ values for various oxygen bearing compounds carrying the inherited ozone isotopic signature, there are presently very few published observations of $\Delta^{17}\text{O}$ for tropospheric ozone itself. Isotopic analysis of tropospheric ozone is particularly challenging due to the low concentration (parts per billion level) and high $[\text{O}_2]/[\text{O}_3]$ ratio found in the troposphere, which complicates the collection and analysis of ozone samples. The paucity of information concerning the $\Delta^{17}\text{O}$ of ambient tropospheric ozone remains a major barrier to the interpretation of $\Delta^{17}\text{O}$ measurements for other atmospheric species. Because ozone is the predominant source of the oxygen isotope anomaly in the troposphere, it is necessary to know the starting isotopic composition of tropospheric ozone in order to extract quantitative information regarding oxidation pathways using an isotopic approach.

We have developed a new method for the collection and subsequent isotopic characterization of ozone using a simple, active air sampler with a nitrite-coated filter in combination with the bacterial denitrifier method for the triple-oxygen isotope analysis of nitrate. This method is light, inexpensive, and easy to implement in nearly any sampling environment, providing researchers with the potential to

monitor variations in ozone isotopes over a network of sites, even in remote or inaccessible areas (e.g., polar and alpine locations, remote ocean, stratosphere, etc.). Additionally, this method does not involve the complex sampling technology utilized in prior studies of atmospheric ozone isotopes and also precludes many of the measurement errors and uncertainties that are associated with these initial investigations. Initial investigations of collection efficiency and isotope transfer, outlined in (Vicars et al., 2012), indicate that this method is sufficiently robust and reliable to be applied to the routine analysis of stable isotope ratios of atmospheric O_3 . However, research into the method is just now moving beyond its preliminary stages and there have been very few measurements made in the ambient troposphere. A better understanding of the nature and scale of spatiotemporal variations in tropospheric $\Delta^{17}O(O_3)$ will require a great number of observations in different contexts and environments, which a sampling campaign across the Atlantic Ocean, from Punta Arenas (53°S) to Bremerhaven (53°N), would provide. In combination with our studies in Dome C, Antarctica during 2011, and our ongoing field measurements in the French Alps, this transect would represent a unique opportunity to extend dramatically the global representation of this variable.

Work at sea

We have sampled tropospheric air continuously onboard *Polarstern* during the ANT-XXVIII/5 cruise. Our ozone sampling apparatus is very light and simple, consisting of a low-volume pump connected to a filter holder with 1/4" PFA tubing. Ozone collection is achieved through the use of a glass fiber filter (Whatman™ GF/A) coated with a nitrite solution. In this technique, oxygen isotopes of ozone are trapped irreversibly in nitrate via the ozone/nitrite oxidation reaction within the filter matrix (Vicars et al., 2012). Filters are then extracted with ultra-pure Milli-Q™ water and stored frozen until analysis at our home laboratory in Grenoble, France. The mean flow rate used for this sampling device was $0.003 \text{ m}^3 \text{ min}^{-1}$ and the normal sampling duration was 24 hours; however, additional collections were performed at shorter durations (6-12 hours) for day/night comparisons. The nitrite-coated filter sampler was operated inside of the OCEANET container. A sampler inlet, consisting of a Teflon pre-filter and filter holder, were employed for the removal of atmospheric particulate matter (PM) upstream of the nitrite-coated filter. Additionally, we have measured the ambient ozone mixing ratio throughout ANT-XXVIII/5 using a standard continuous ozone monitor (2B Technologies™, Model 205), thus allowing for an estimation of collection efficiency for the ambient filter samples. The ozone monitor was also connected to a Teflon pre-filter and both sampler inlets were installed on the outside of the OCEANET container (Fig. 8.1).



Fig. 8.1: Sampling inlets for the nitrite-coated filter sampler and continuous ozone monitor installed outside of the OCEANET container

8. Measurement of the oxygen isotope anomaly (^{17}O -excess) of ozone

We have also carried out atmospheric PM collection using a high-volume air sampler (HVAS), which was installed on the monkey deck (Fig. 8.2). Atmospheric PM sampling was conducted in order to investigate the link between the isotopic composition of ozone and that of nitrate, which is present in the marine boundary layer at a concentration much lower than that of ozone. This sampling program is essentially identical to the one carried out by Samuel Morin in the spring of 2007 onboard the *Polarstern* cruise ANT-XXIII/10 (Morin et al., 2009). The HVAS draws air at a flow rate of $1.1 \text{ m}^3 \text{ min}^{-1}$ through a four-stage cascade impactor (Tisch Series 230), which is loaded with pre-cleaned slotted glass fiber (GF) filters (Tisch TE-230GF, $12.7 \times 17.8 \text{ cm}$) and a larger GF backup filter (Whatman GF/A, $20.3 \times 25.4 \text{ cm}$). The cascade impactor aerodynamically fractionates particles into five size classes with cuts at 7.2, 3.0, 1.5, 0.95, and $0.49 \mu\text{m}$ aerodynamic diameter (Da). In order to ensure an amount of nitrate sample sufficient for isotopic analysis (approximately 100 nmol) in each extract solution, the filters of the first two stages and those of the last three stages are combined into two separate samples, one comprised of the total supermicron (Da > $1 \mu\text{m}$) particle fraction and the other containing all submicron (Da < $1 \mu\text{m}$) particles. Sampling duration for the HVAS was typically in the range 24-48 hours for this experiment, although it was decreased to approximately 12 hours during the Saharan dust event of 30 May – 1 June.



Fig. 8.2: The HVAS, "frequent flyer," installed on the monkey deck

Preliminary Results

Ambient ozone mixing ratio varied in the range of 13 – 55 parts per billion (ppb) during ANT-XXVIII/5 with an average value of $28.8 \pm 8.0 \text{ ppb}$ (Fig. 8.3). The highest values (> 50 ppb) were observed in the northern latitudes when *Polarstern* approached the European subcontinent, reflecting the effect of anthropogenic influences on the ozone content of the atmosphere. Lowest mixing ratio values were observed during the southernmost portion of the cruise, where the continental influence is minimized. Nitrite-coated filter samples were typically collected at durations of 24 hours during the southern section of the cruise and in the intertropical convergence zone (ITCZ); however, when ozone mixing ratio was

observed to exceed 40 ppb, the sampling duration was reduced to 12 hours in order to make daytime/nighttime comparisons. In sum total, 40 nitrite-coated filter samples and 22 sets of atmospheric PM samples were collected during the cruise.

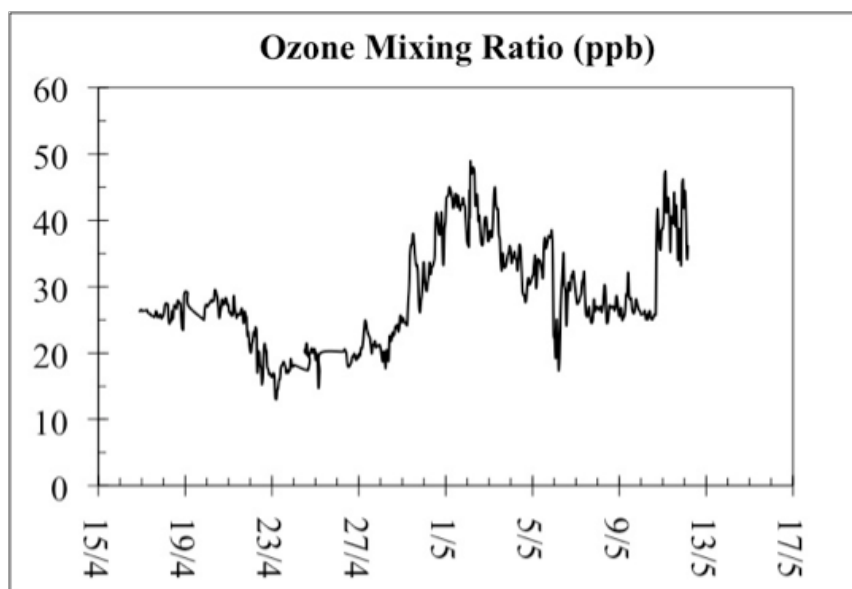


Fig. 8.3: Hourly averages of ambient ozone mixing ratio during ANT-XXVIII/5

Data Management

The majority of samples collected during ANT-XXVIII/5 will be processed and analysed at our home laboratory in Grenoble. Ozone filter samples will be extracted using sulfamic acid, which is necessary for the removal of excess nitrite ion before isotopic analysis. The triple-oxygen isotope analysis of the nitrate produced on the filter during the ozone/nitrite reaction will be accomplished using the bacterial denitrifier method followed by isotope-ratio mass spectrometry (IRMS), which directly yields the $\Delta^{17}\text{O}$ value transferred from ozone. Atmospheric PM samples collected using the HVAS will be extracted in pure water and also analysed using the bacterial denitrifier method. The isotopic compositions of atmospheric nitrate and ozone will be used for quantifying $\Delta^{17}\text{O}$ transfer from ozone. We expect the majority of chemical analyses and data processing to be accomplished within one year (May 2013). Once completed, this data will likely be published as a component of a larger geographical and temporal survey of the isotopic composition of ozone. We are willing to share this data in collaboration with other cruise participants.

9. CULTURE EXPERIMENTS ON THE ENVIRONMENTAL CONTROLS OF TRACE METAL RATIOS (MG/CA, B/CA, U/CA) RECORDED IN CALCAREOUS TESTS OF ARCTIC DEEP-SEA BENTHIC FORAMINIFERA

Erik Wurz

AWI

Jutta Wollenburg (not on board)

Objectives

Newly developed high-pressure aquaria have recently facilitated the first efficient cultivation (producing offspring) of our most trusted palaeodeep-water recorders *Fontbotia wuellerstorfi* and *Uvigerina peregrina*. In different experimental set-ups the same facilities will be used during the ANT-XXVIII/4 and ANT-XXVIII/5 cruise to cultivate these foraminifera and associated species in waters with different carbonate chemistries to establish the first species-specific trace metal calibration curves for the Antarctic Ocean. Therefore, short sediment cores from 1,300 to 1,500 m water depth must be collected and transferred into high-pressure aquaria as well as atmospheric-pressure aquaria.

Work at sea

Sediment sampling was carried out using a standard 8-tube multicorer (MUC) with an inner tube diameter of 10 centimeters. Three MUCs were successfully deployed at 3 stations (1,540 to 1,571 m water depth) southwest of Elephant Island. Immediately, after recovery the MUC tubes were transferred into push corers and those into the aquaria. By this method, we have successfully filled 5 high-pressure aquaria that are now cultured at pressures of 145 to 150 bar, and 10 aquaria running at atmospheric pressure.

The aquaria are operated in a cold laboratory running at 0 °C. Each aquarium (high-pressure and atmospheric pressure aquaria) was connected to its own supportive seawater system. Hereby high-pressure pumps and a chain of in- and outlet valves maintain *in-situ* pressure and assisted by peristaltic pumps a constant seawater flow through the high-pressure aquaria. The seawater used in the system was sampled from 1,200 to 1,500 m water depth. Seawater sampling was accomplished using an SBE 3,2 carousel water sampler operated by Th. Badewien from ICBM.

The pH of the running systems is constantly noted and adjusted by a pH-control system and connected buffer pumps. Oxygen is measured every 4 hours. Once a week, a suspension of algae was added to the seawater inflow as a food supply.

Preliminary Results

The aquaria and seawater circuits will be maintained during the expedition ANT-XXVIII/5 until on May 16, 2012 the systems can be moved to the laboratories at the Alfred-Wegener-Institute in Bremerhaven. Preliminary results will be obtained approximately 6 months after the end of ANT-XXVIII/5.

10. MOLECULAR BASIS OF CLIMATE SENSITIVITY IN ANTARCTIC FISH: MITOCHONDRIAL FUNCTIONING AND ITS IMPLICATION FOR IONIC AND OSMOTIC REGULATION

Nils Koschnick, Tina Sandersfeld, AWI
Erik Wurz, not on board:
Magnus Lucassen, Hans-Otto Pörtner

Objectives

Increasing CO₂ in the atmosphere causes both, ocean warming and acidification. Due to its pervasive impact on all biological processes, temperature is a crucial abiotic factor limiting geographical distribution of marine ectothermal animals on large scales. Additional environmental factors like increasing PCO₂ and the concomitant drop in water pH are thought to narrow the thermal window, as they are believed to act on the same physiological mechanisms. Thermal adaptation and phenotypic plasticity, which define the thermal niche and the responses to fluctuating environmental factors, are ultimately set by the genetic interior of the organisms. Adaptations to the extreme cold appear to be evolved at the expense of high thermal sensitivity. Mitochondrial functioning and maintenance resemble a key functional trait, as it is directly related to the aerobic performance windows of animals. Example studies on mitochondria from Antarctic fish suggest that mitochondrial functioning underwent significant adaptations upon evolution to extreme cold. Our findings of elevated capacities of respiratory chain components and uncoupling proteins in Antarctic eelpouts upon warm acclimation suggest the use of acclimation pathways different from those in temperate fish. Furthermore, we identified a molecular network, responding sensitively to warming beyond the realized ecological niche and mediating large rearrangements in energy metabolism.

The interrelation of ion regulation and energy demand becomes obvious in branchial mitochondrial-rich cells, where the main ion pump, the Na⁺/K⁺-ATPase, is concentrated, too. Tight regulation of this process with a strong impact on whole animal energy budget has been shown both in response to temperature and CO₂. Ocean acidification is compensated for by an efficient ion regulatory system. With respect to temperature effects, different strategies in the use of active and passive strategies of pH regulation are discussed for cold-adapted and temperate species. As hemoglobin-less icefishes are characterized by larger blood volume and flow due to limited oxygen transport capacity, consequences for the passive transepithelial transport of ions may be postulated.

Here, we aim to characterise the branchial energy budget and ion regulatory system in gills in relation to the allocation of energy by mitochondria upon relevant environmental factors in an array of different Antarctic fish groups, to distinguish common principles and specific climate sensitivities in the light of the ongoing climate change.

Work at sea

On the cruise leg ANT-XXVIII/4 different Antarctic fish species were caught by use of baited traps and by bottom trawls. These fish were kept in an aquarium container to be transported to the AWI's aquarium in Bremerhaven. Most of these animals are highly adapted to the cold temperatures of the Southern Ocean, but the technical equipment of *Polarstern* allowed maintenance of these conditions. To guarantee good water quality, the aquarium water had to be exchanged several times a day. Thus, huge water volumes were cooled down and water quality was monitored continuously.

Besides the maintenance of the aquarium container, laboratory work is carried out. The capacity and temperature sensitivity of the ion regulatory system was characterised in isolated fish gill (at the AWI). For this purpose, tissue extracts were prepared and photometric enzyme assays were carried out. This data will be verified by additional measurements in the AWI's laboratories in Bremerhaven.

Preliminary results

In total about 80 individuals of eight different fish species (*Ophtalmulycus amberensis*, *Champsocephalus gunnari*, *Notothenia coriiceps*, *Notothenia rossii*, *Lepidonotothen nudifrons*) and 250 specimen of three different octopod species (*Paraledone* spec.) were transported to the AWI's aquarium in Bremerhaven. The fish will be used for temperature dependent growth experiments. These experiments shall contribute to understand temperature sensitivity of Antarctic fish and the effect of temperature on the Antarctic fish energy budgets in the framework of climate change. For this purpose, different organismic levels will be analysed by physiological and molecular biological means to characterise performance-limiting processes at elevated temperatures and different CO₂ concentrations.

11. SEA TRIALS AND VALIDATION OF THE MULTIBEAM HYDROSWEEP DS-3

Saad El Naggari¹,
Ralf Krockner²,
Jörn Ewert³

¹F. Laeisz
²AWI
³ATLAS Hydrographics

Objectives

The main objectives of the sea trials were to further test and validate the forward looking capability of the newly developed beam-former (SPM-II Module) of the upgraded sonar system HYDROSWEEP DS-3 from ATLAS Hydrographic, Germany, and to verify its deep sea performance after the hardware and software modification.

The first version of the DS3 system was installed in October 2010 and tested during *Polarstern* cruises ANT-XXVII/1 and ANT-XXVII/4. The test results led to significant hardware and software modifications especially to install the forward looking functionality. The forward looking technology from flash mounted transducers was especially developed by ATLAS to online determine the mean sound velocity and to observe in advance the sea floor topography in order to provide support for navigation and for scientific purposes. The new developed beam-former SPM-II was initially tested in November 2011 during ANT-XXVIII/1.

Work at sea

In the first part of the cruise from Punta Arenas to Las Palmas de Gran Canarias the sonar system Hydrosweep DS3 was operated by ATLAS engineer. Updates in software and hardware were installed and the system's settings were optimized during profile measurements.

The sonar system can be operated on four computers. The Master Control PC (mcpc1ds3) and a secondary control PC (mcpc2ds3) are installed in HS/PS office. Secondary control PCs are also installed on the bridge (mcpc3ds3) and in winch room (mcpc4ds3). At the beginning of this cruise the operation system Windows XP was updated to Windows 7 (64 Bit) on all these computers. Furthermore a new version of Control Module for controlling electronic devices and a new version of the operator software (ATLAS Hydromap Control – AHC) was installed. For online visualization and data archiving the software package Hypack is used, which was also updated to 2012-Version, 64 Bit. Control PCs 1, 3 and 4 got new ATI graphic cards. The old graphic card from PC 1 was installed in PC 2.

Sea trials were started with hardware components TBF (Transmitting Beam Former – old version) and SPM MK-II (Signal Processing Module – new version) until leaving the bathymetric profile measurements at 35° 00' W / 20° 40' S. After that survey the old TBF was changed to a modified TBF.

To adjust and optimize the sonar's parameters for different survey modes varying seafloor characteristics and especially varying depths and slopes were intended to be profiled. At the beginning of the cruise, medium depths on the shelf off

11. Sea trials and validation of the multibeam Hydrosweep DS-3

Argentina were surveyed. Heading to North-East, the cruise led to the deep sea with both flat and fractured topography. At 35° 00' W / 20° 40' S the steep slopes of guyot "Davis Bank" were surveyed.

To obtain precise water depths, the mean sound velocity in water column is necessary. During the cruise several CTD casts have been accomplished by another group and provided for import in ATLAS Hydromap Control and Hypack Package.

As new sonar feature the Multi-Ping Mode was installed. In this mode two pings are sent simultaneously, one looking slightly backwards one slightly forward. In this mode double resolution in along track direction will be achieved which therefore avoids gaps between consecutive profiles at higher ship speed.

As another feature the Chirp Mode was installed. In this mode the frequency modulated signal will be evaluated, which leads to better signal detection of the outer beams and so to larger swath widths. But the parameter setting for this mode was not developed and evaluated satisfactory during this cruise. As consequence this mode cannot be used during scientific surveying but must be part of further developments and adjustments.

During the second part of the leg from Las Palmas to Bremerhaven the actual configuration of the Hydrosweep DS3 system was evaluated.

As test area for the Forward Looking Functionality the Ampère Seamount was surveyed from 07 May 2012, 22:50 UTC until 08 May 2012, 07:20 UTC. A 7.2 nautical miles long profile from 35° 06' N / 13° 02' W at 1770 meter water depth to 35° 03' N / 12° 54' W at 130 meter water depth was surveyed four times uphill and three times downhill with varying parameter settings.

1st up: 45° steering, Chirp mode on
1st down: 45° steering, Chirp mode off
2nd up: 35° steering, Chirp mode on
2nd down: 35° steering, Chirp mode off
3rd up: 20° steering, Chirp mode on
3rd down: 20° steering, Chirp mode off
4th up: 20° steering, Chirp mode on, variation in stewart configuration
4th down: 20° steering, Chirp mode off, variation in stewart configuration

This area was surveyed because its steep slopes are a challenge for all multibeam sonar systems. Furthermore this sea mount was already well charted during previous cruises with previously installed sonar systems. In comparison to these existing data, the quality and resolution of the new data will be assessed.

North-West of the base of Ampère Seamount a second profile already surveyed during ANTX XVIII/1 in November 2011 was re-measured to compare data sampled with previous settings with older beam-formers with the new situation. The profile with length of 13.2 nautical miles is situated between position 35° 13' N / 13° 02.8' W and position 35° 18.6' N / 13° 17.4' W.

At the end of the cruise from 14 May, 18:50 UTC to 21:09 UTC a 8.9 nautical miles long profile between position 54° 12.8' N / 7° 14.5' E and position 54° 11.3' N / 7° 27.4' E (south of island Helgoland) was surveyed. The survey was conducted in water depths between 60 and 21 meters to optimize the sonar system settings for shallow water.

In addition during all surveys the systems runtime stability was observed to confirm a continuous operating.

When the new sonar Hydrosweep DS-3 was installed in October 2010, a user manual was written, to assist non bathymetry specialists operating the echo sounder. This manual was updated during ANTXXVIII/5 cruise due to the numerous changes in the software applications.

Results

The sonar system with new hardware components TBF and SPM MKII as well as new software applications ATLAS Hydromap Control and Hypack was not running during a longer period. For this reason the experience about the systems stability is not significant and must be confirmed during a longer scientific cruise. During this cruise no system failures that force a restart or any kind of manual error handling has been detected. Unfavourable sea floor conditions like steep slopes have been detected without interruptions, miss detections or any other kind of errors.

The improvement of precision and resolution of depths measured with new system Hydrosweep DS-3 compared to the old system Hydrosweep DS-2 was already pointed out in previous reports. Due to the new sending and receiving beam formers the precision and resolution of depths could be improved once more, especially in shallow waters.

As can be seen in Fig. 11.1 there is a gap in the bathymetry profiles. Such gaps have frequently been detected during the cruise and seem to be produced by Transmitting Beam Former, when the depths are changing and the system is adjusting the internal parameters for the new environment. These gaps should not occur and need to be eliminated by further developments of ATLAS.

The new Signal Processing Module allows the pre-adjustment of parameters to reduce the effect of beam dependent offsets and uncertainties. These so called "tramlines" could nearly be eliminated in the center of the profiles and in the area half of swath width on port and starboard side. In shallow water less than 100 meter this effect still exists and might be subject of further developments.

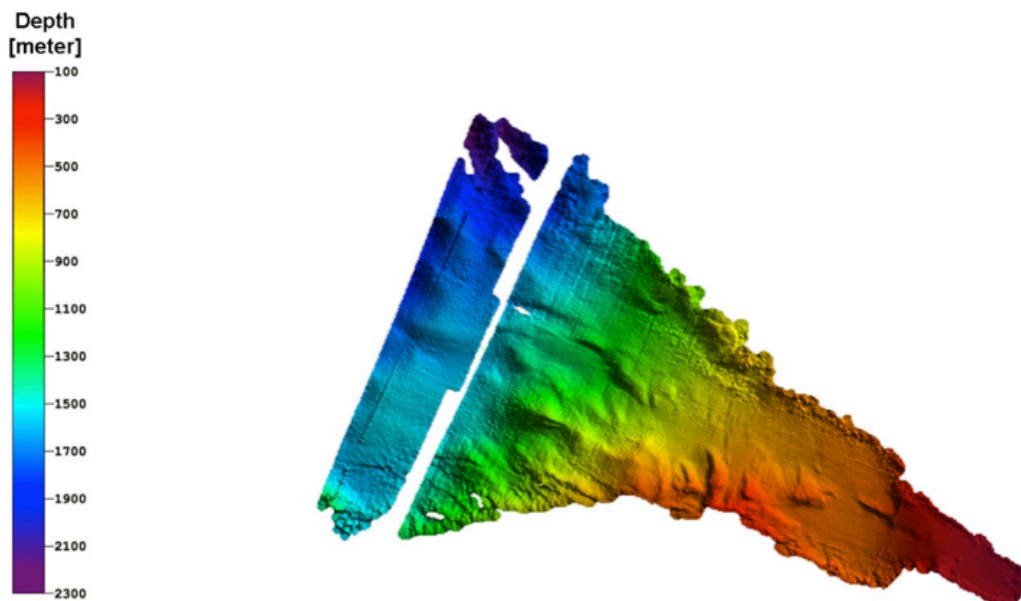


Fig. 11.1: Single profile downhill the Ampère Seamount without Chirp Mode

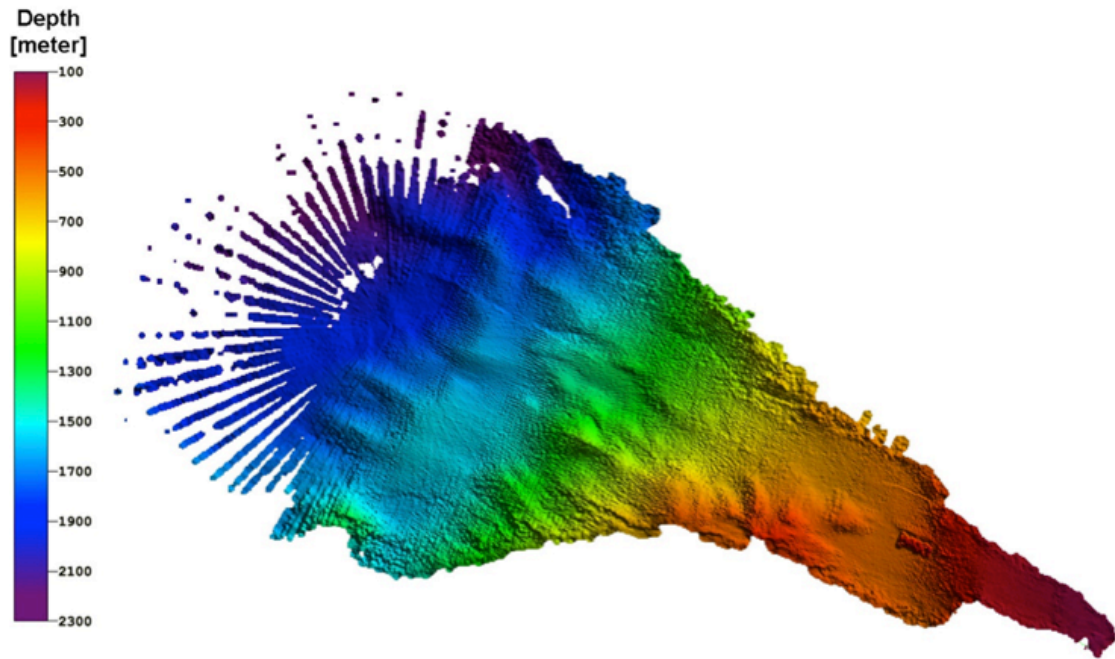


Fig. 11.2: Average of 5 profiles with and without Chirp Mode and varying angles in forward looking

Another feature of new Signal Processing Module is the Chirp Mode. In Chirp Mode changing frequencies at signal transmission can be evaluated during receiving that signal for better detection of outer beams. This decreases the noise for outer beams and increases the detectable swath width. But as can be seen in Fig. 11.2 which was created from depths measured with Chirp Mode that there is a roughness upon the data which is not observable for measurements without that mode as can be seen in Fig. 11.1. Chirp mode must also be subject of further developments. Until this mode is not working proper it should not be switched on.

The participation of ATLAS engineer during the cruise was planned to further develop the Forward Looking Functionality of the Hydrosweep sonar. Unfortunately, the investigations during the cruise do not meet the expectations. Initially it was meant that a full swath width of 90 degree could be sent and received 45 degrees forward. This swath angle was seen as too optimistic during further developments and was successively decreased. At the beginning of the cruise the angle was reduced to 4 degrees. Sampled data and investigations during this cruise led to the result that this functionality will not yield to the desired results. As a consequence not only the forward looking to support the ships navigational safety is available. Additionally the hydroacoustically determination of mean sound speed is not possible.

Finally it can be stated, that the update of hardware and software components have improved the quality of measured depths. The possibility of parameter adjustment makes it possible to further improve the precision of depths in the future.

On the other hand the failed development of the forward looking sonar forces the development of other techniques to provide the guaranteed functionality.

12. DEPTH-PROFILE OF ZIRCONIUM, VANADIUM, TITANIUM AND MOLYBDENUM IN SEAWATER-ADSORPTION STRIPPING VOLTAMMETRY, AN INTERESTING ANALYTICAL TECHNIQUE

Alexandre Batista Schneider,
Andrea Koschinsky (not on board)

Jacobs University

Objectives

To determine the concentration, input, distribution, boundaries and sinks of zirconium, vanadium, titanium and molybdenum in seawater by voltammetry.

Work at sea

During the Cruise ANT XXVIII/5 with the *Polarstern*, I was mainly occupied with sampling. I was just interested in the stations, at which I could have a whole depth-profile of the water column in relation to the concentration of zirconium (Zr), vanadium (V), titanium (Ti) and molybdenum (Mo). Thus, I just took the samples the CTD collected from the surface up to the seawater bottom, or at least those samples, collected at stations deeper than 2000 m. In this approach, following sites were sampled: 298, 304, 306, 308, 310, 314, 318, 319, 322 and 328 (see station-list). I took three different aliquots for each collected depth, 500 mL for the chromium-speciation by voltammetry, carried out by colleagues at the Jacobs University Bremen, other 1000 mL for posterior determinations of hafnium, niobium, rare earth and other important inorganic components by ICP-OES and ICP-MS at the Jacobs University as well. Finally, I took other 500 mL for the voltammetric determination of Zr, V, Ti and Mo by me. For most of the mentioned and not cited elements, the depth-profile is decisive for understanding the distribution, the relationship between this elements and sinking particles (and if they are related either to particulate matter or to colloids and if they sediment or rather stay in suspension), and very important, try to find out the main sources of these elements in the sea. Moreover, besides the influence of rivers and estuaries, dust and anthropogenic input directly into the water surface, the hydrothermal vents, the so-called "black smokers", are also important sources directly at the sea's bottom. Hence, the sampling sites along the Mid-Atlantic-Ridge played an important role linked to the appearance of some trace elements into the water column. Other sources like dust from the Saharan desert could be an important source for Chromium. Thus, the samples collected at the sampling sites along the Africa's coast are very interesting for the further chromium-speciation. Physical and chemical differences like conductivity, temperature, pH-values, redox potential and oxygen content could be of great significance trying to understand the results evaluated by us in the near future. Some of the analytics are particle reactive elements, other rather redox-sensitive elements and other behave conservatively in the water column. The collected samples had to be kept frozen during the

cruise. Some were filtered and acidified by me on Board and will be compared with filtrations on the land. Besides sampling and sample treatment, I measured pH and redox potential of all the samples taken by me. I intended to carry out some measurements by voltammetry on the ship during the cruise, but due to analytical problems they weren't possible. But the conservation of the samples will enable all the voltammetric measurements to be carried out partially in Bremen, partially in Santa Maria, Brazil.

Preliminary (expected) results

Laboratory mixing experiments have been used by us to investigate the behaviour of Ti, Zr, V and Mo during estuarine mixing. Our preliminary experiments to simulate the mixing in the Elbe and Rhine estuaries have yielded interesting results that had not been previously investigated. The enrichment of both Ti and Zr at 50:50 river to sea water mixture will especially be a subject of further investigation in other experiments. Both Ti and Zr show a non-conservative mixing behaviour with similar surface distributions because of their similar chemistry (both are group IV elements) during the mixing. Ti and Zr are strongly particle reactive elements hence are rapidly removed from solution at low salinities during mixing in both rivers. The concentrations of both Mo and V are highest in sea water suggesting that there is very little estuarine removal of the two. Therefore adsorption seems to have a negligible effect in regulating the concentrations of the two elements compared to Ti. Mo also shows a general conservative behaviour during mixing. Further similar experiments with water from the Weser River and the Elbe River are currently on-going in our lab and these will be compared to these results. ICP-OES/ICP-MS measurements of the mixtures will be performed and compared to these results and additional measurements for conservative elements (Sr, Na, Ca, and Mg) will be carried out to verify if the mixing was indeed linear.

The focused elements belong to the group of transition metals and are characterized by small ionic radii and high charges (mostly tetra-, penta- and hexavalent) in marine systems. The elements Ti, Zr are also grouped as high-field strength elements (HFSE). These HFSE have a strong tendency towards hydrolysis, are highly particle reactive, and are rapidly removed from solution by interaction with surfaces of sinking particles. This behaviour leads to very low truly dissolved concentrations of these elements in natural waters and a strong impact of colloids and particles on their dissolved concentrations.

Dissolved Titanium is present in seawater in very low concentrations and ranges e.g. between 4-8 pM at the surface and 200-300 pM near the bottom of the North Pacific (Orlans, Boyle, & Bruland, 1990). Titanium is particle-reactive and has a short residence time, similar to other hydroxide-dominated elements like aluminium and iron. However, unlike Al, dissolved Ti is depleted in surface waters and increases with depth leading to enriched bottom waters. Aeolian and fluvial input in surface waters and benthic fluxes and deep water remineralisation at depth (Orlans, Boyle, & Bruland, 1990) (Skrabal, 2006) are assumed to be sources for Ti. As for Ti, concentration data for Zr display a general increase with depth in water column profiles from the Pacific and Atlantic oceans (Godfrey, White, & Salters, 1996 and Firdaus, Norisuye, Nakagawa, & Sohrin, 2008).

In contrast to the HFSE, which typically have only one oxidation state (+4 and +5, respectively), V and Mo can display variable oxidation states in marine systems. Vanadium can be present as V(IV) and V(V) whereas Mo can display as Mo(V) and Mo(VI). Different redox species show different affinities towards particles and

ligands in solution leading to a variation with respect to their bioavailability and biogeochemical reactivity. Therefore, redox conditions display a major control on the distribution of these redox-sensitive trace metals. For V, only oxidation state +5 is stable in oxic seawater at neutral pH. The fully hydrolysed vanadate species such as HVO_4^{2-} , H_2VO_4^- and the complex NaHVO_4^- predominate (Middelburg, Hoede, Van der Sloot, Van der Weijden, & Wijkstra, 1988). Vanadate is relatively poorly reactive with major dissolved cations and neutral particles. Complexation with organic matter does not seem to have a significant effect on its behaviour (Jaendel, Caisso, & Minster, 1987). Average concentrations of V in the ocean range between 34 to 45 nM (Emerson & Husted, 1991) and display a nearly conservative depth profile with a slight surface water depletion, which is more pronounced in the Pacific Ocean (Collier, 1984) than in the Atlantic Ocean (Jaendel, Caisso, & Minster, 1987 and Middelburg, Hoede, Van der Sloot, Van der Weijden, & Wijkstra, 1988). Vanadium plays an important role in biological processes as an enzyme component for microorganisms. Sources of V include riverine and atmospheric inputs as well as exchange with deeper water. As V is preferentially adsorbed in its reduced form vanadyl, VO_2^{+} , bottom water with low oxygen content displays a major sink for V, where it is taken up into anoxic, organic-rich sediments (Emerson & Husted, 1991). Molybdenum exists in oxic water with pH above 6 as Mo(VI) and forms oxyacids MoO_4^{2-} . However, a recent study found that Mo is also stable in natural waters as Mo(V) and contributes with 0 to 15 % of the dissolved Mo in the Peconic River estuary (Wang, Aller, & Sanudo-Wilhelmy, 2009). The concentration of Mo in the open is nearly constant with depth at ~ 106 nM (Sohrin, Isshiki, Kuwamoto, & Nakayama, 1987). As concentration of Mo in seawater are 100-1000 times greater than that of other trace metals it greatly exceeds biological requirements and therefore shows no surface depletion (Collier, 1985). Another study (Sohrin, Isshiki, Kuwamoto, & Nakayama, 1987) explains that oxyacids hardly form complexes with organic ligands, hence a smaller fraction can be adsorbed onto organisms and organic particulate matter in surface waters. Therefore a significant surface depletion does not take place.

The voltammetric methods for the determination of Zr, V, Ti and Mo in the samples taken during the cruise with *Polarstern* were optimized by me in Santa Maria and in Bremen. The analytical method for the determination of these analytes is Adsorption Stripping Voltammetry, AdSV. The stripping voltammetry methods are the most capable electro analytical techniques for the traces and speciation analysis. The extraordinary high sensitivities are based on the previous preconcentration of the analyte before its determination. As the preconcentration as well the determination occur at the same work-electrode (Hanging Mercury Drop Electrode, HMDE) and without change of the solution-vessel, the risk of systematic errors followed of contamination or escape of the analytes are very low. The term "stripping" means that, during the determination, the product of the former preconcentration-step is re-dissolved in the original solution from the work electrode. We call Adsorptive Stripping Voltammetry (AdSV), when the analyte in an appropriate form, like as a coordinated complex, adsorbs at the work electrode during the preconcentration step (during electrolysis). This is an important complement to the electrolysis, once the Stripping Voltammetry becomes also useful for those elements which react irreversibly with the electrode or, due to a weak amalgam-formation with the mercury-work-electrode, cannot neither be preconcentrated at the electrode-surface nor be determined during stripping. This is the case of these elements studied by us, Zirconium, Vanadium, Titanium and Molybdenum. An important field of the application of the AdSV is the determination of trace of elements in aqueous

12. Depth-profile of Zr, V, Ti and Mo in seawater-adsorption stripping voltammetry

samples. In most cases, the quantification limit is around intermediates or lower ng L^{-1} (ppt). Thus, the AdSV is, beside techniques coupled to mass spectrometry and neutron activation analysis, one of the most sensitive techniques of the instrumental analysis. These methods were previously applied by us on digested samples (by UV-irradiation), collected during the cruise 81/1 with the FS Meteor, which were kept frozen. Moreover, we analysed a certified reference seawater, NASS-5, which was collected in the North Atlantic at a depth of 10 m and 35 km southeast of Halifax, Canada. The Zirconium concentration found by us is in the same range of that published by Firdaus et al. (2007), who found a concentration of nearly 183 pmol L^{-1} Zr (nearly 16 ng L^{-1}) in the same certified reference material.

Data management

After evaluation, the results will be compared with other analytical techniques like Inductively-coupled-plasma with mass detector and atomic absorption spectrometry, published in scientific magazines and they will be linked to other data collected by other researcher after other cruises in other regions, in a coordinated way inside the wide GEOTRACES community.

13. INVESTIGATION OF THE NUMBER DENSITY, PROPERTIES AND SOURCES OF ICE NUCLEI IN THE MARINE ATMOSPHERE

Monika Kohn¹,
Heinz Bingemer¹ (not on board)

¹IAU

Objectives

Much of the global precipitation is formed by super cooled droplets in mixed-phase clouds. In this project aerosol particles with the ability to grow ice crystals, so called "ice nuclei" (IN) are investigated. These particles have a special surface characteristic that allows forming ice crystals, provided that the air is cold enough (below freezing) and is supersaturated with water vapour. IN are rare among the atmospheric aerosol particles (only 1 in 10^4 – 10^5). Even though a variety of substances like mineral and volcanic dust, bacteria and plant debris are known to act as IN, there is still a lack of information on their (bio) geographical distribution and the climatology of their number concentration. The transatlantic transect is unique for ship-based IN measurements because it offers a broad spectrum of different atmospheric environments to obtain data of the distribution as well as sources of ice nuclei, ranging from pristine South Atlantic air masses, tropical biomass burning, and mineral dust events to polluted northern hemispheric air, including biologically active upwelling areas.

These experimental data are used to parameterize and implement IN into global models to better understand and predict cloud processes and their impact on earth's climate.

Work at sea

During ANT-XXVIII/5 samples of aerosol particles were collected daily off-line with the electrostatic aerosol collector (EAC) on silicon substrates aboard *Polarstern*. The measurements took place, on top of the aerosol container of *Ift Leipzig* on the monkey-deck and in the crow's nest, depending on the intensity of sea spray and weather conditions. Aerosol particles were sampled from an atmospheric air volume between 2 and 20 Liters according to the current particle size distribution and number distribution as detected by a portable Optical Particle Sizer. On this cruise leg about 100 samples were collected. Additional samples were taken during the dust plume in the area east of the Cape Verde Islands for a higher temporally and geographical resolution of the data.

Data and samples

Samples collected on *Polarstern* will be taken to the *Goethe-University of Frankfurt* for the subsequent analysis and the investigation of the ice nuclei number density with the ice nucleus counter FRIDGE (Frankfurt Ice Deposition Freezing Experiment).

13. Invest. of number density, properties and sources of IN in marine atmosphere

The samples are analysed with the static vacuum vapour diffusion chamber at subfreezing temperatures (-8°C to -18°C) and super-saturation (100-120 % in respect to ice) to obtain the IN number concentration. The chemical composition and morphology of IN is investigated by environmental scanning electron microscopy (ESEM) in cooperation with the *Technical University of Darmstadt*. Instrumentation (Aerodynamic Particle Sizer, Scanning Mobility Particle Sizer) of the research group from *IfT Leipzig* provide information about general physical and chemical properties of the atmospheric aerosols. This information is used to parameterize IN abundance and nucleation properties to achieve a better understanding in the formation of clouds and their influence on climate.

Expected results

Since our filter samples will be analysed at the home laboratory in Frankfurt, we can only speculate about our results at this point. As a result of the Saharan dust event a peak in IN concentration is expected for this period, because mineral dust is known to activate very well as IN. Assuming there will be no artefacts due to sea salt within the FRIDGE analysis, a relatively lower IN activation is expected for pristine Atlantic air due to the low aerosol particle concentration in the marine boundary layer. Backwards trajectories provided by the meteorological service aboard *Polarstern* will be used to analyse the source of the air masses investigated.

Data management

The data processing will be carried out at IAU. This will take several months. After post processing the data sets are available for other cruise participants after request.

14. DEVELOPMENT OF A WEB APPLICATION FOR SCIENTIFIC DEVICES AND SYSTEMS DURING ANT-XXVIII/5

Peter Gerchow, Antonia Immerz AWI

Objectives

The aim of the project was to develop a web application to generate configuration files necessary to send sensor data of measurement devices stored in the DShip-System on board *Polarstern* via the computer network.

The DShip-System on board *Polarstern* gathers scientific raw data obtained from the different available measurement devices such as echo sounder, navigation systems, and thermosalinograph among others. The data is stored in databases and visualized online as well as stored for a later offline extraction on board or back at the institute.

Furthermore it is possible to spread current measurement data via the computer network. Here for the NMEA-Standard is used which was defined by the National Marine Electronics Association (NMEA) to realise communication between navigation devices on ships. The corresponding module in the DShip-System is called NMEA-Client.

With the NMEA-Client specific sensor data of the available measurement devices is represented in a so-called telegram. The telegram is composed of comma separated text lines which contain the respective data to be sent to other devices or computers via the network.

To configure the telegrams various parameters like desired sensors, recipients of the telegram, sending interval and format of the data have to be specified in a configuration file. As this requires some prior knowledge regarding the NMEA syntax the configuration files are often written by the system administrator.

Preliminary Results

During this project a web application, the so-called NMEAMaster was created with which users are able to generate the configuration file using a graphical user interface (Fig. 14.1). Specific sensors are selected from a list and additional parameters can be specified. The configuration file is then generated by simply clicking the button. Apart from this existing configuration files can be loaded into the interface to be updated and saved.

An NMEA-File consists of meta information such as recipients of the telegram, sending frequency of sensor data and timeout definition of pending data. The main

part of an NMEA file are the so-called descriptions consisting of any desired amount of values each respectively defining one sensor whose data is to be transmitted.

The web application is divided into the subsequently presented pages.

Entry

The entry page is the first page the user is navigated to when entering the application website. He is requested to either create a new NMEA file or open an existing NMEA file for editing. When choosing to generate a new NMEA file the application creates an empty NMEA object, with the parameters to be filled in the following pages. For loading an existing NMEA file the application parses all data in the given file and creates a corresponding internal representation prefilling the parameters with the file data. For this purpose regular expressions are used which can be defined in a separate configuration file to maintain flexibility towards later changes of the NMEA Standard.

After choosing the appropriate option the user is guided to the overview page.

Overview

On the overview page the user sees a complete listing of the current parameters for the NMEA file. From here the pages for editing meta-information and descriptions can be accessed by pressing the corresponding buttons. Listed descriptions can be rearranged and deleted and also modified. Furthermore the page exhibits the functionalities to save the finished NMEA file on the DShip server. The file can also be stored on the local computer.

Meta-information

As described above the meta information refers to send frequency of sensor data and recipients. Various recipients can be configured on the meta information page.

Descriptions

Descriptions consist of general parameters such as separator for transmitted values in the telegram and a prolog naming the telegram. The main section of the page is reserved for defining the values of descriptions. Here for the user can choose from a list of devices. After choosing the appropriate device the list of sensors available for the device and data formatting options are listed. The lists and formatting options are automatically generated from an XML file containing the complete list of device definitions configured in the DSHIP-System. As numerous values can be added, similar to the descriptions list on the overview page, functionalities of rearranging, deleting and modifying the values are offered.

Help

The web application contains a help page explaining parameters. By clicking on links on the pages for editing the NMEA file the user is directly guided to the appropriate help section.

Features

The application was designed using object orientation principles. A configuration file for key words, configuration parameters such as email address of the system administrator, file paths etc. was created to enable facilitated configuration of the application in case system parameters or NMEA file definitions change.

The web application will also be installed on the scientific ship *Heincke* and was there for conceptualized to be run on both systems without any modifications.

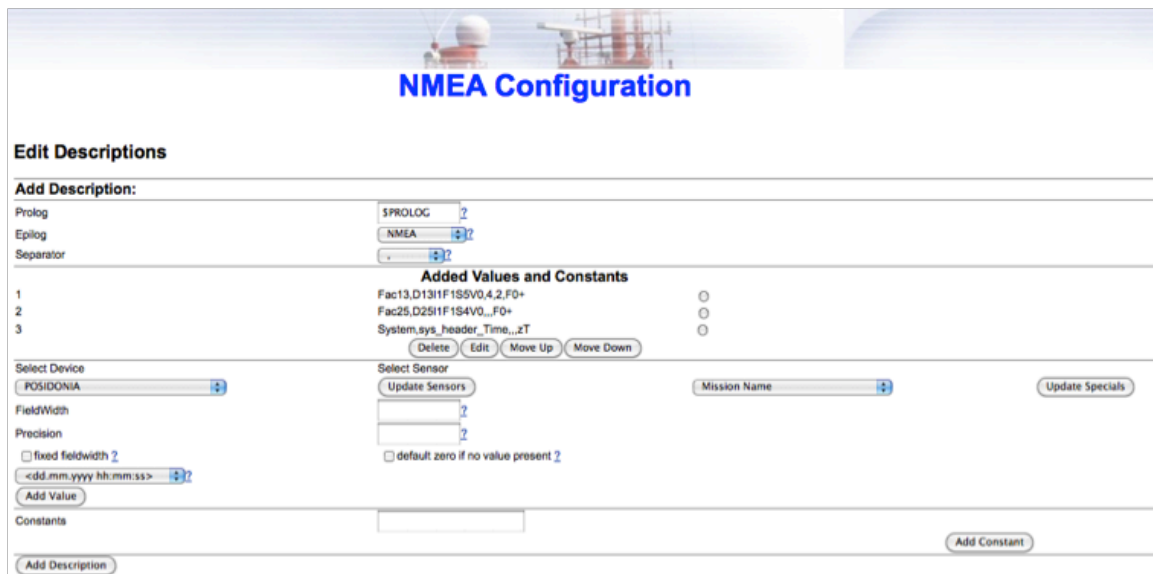


Fig. 14.1: Page of NMEAMaster for editing descriptions

15. REFERENCES

- Agrawal, Y.C., A. Whitmire, O. A. Mikkelsen and H. C. Pottsmith (2008). Light scattering by random shaped particles and consequences on measuring suspended sediments by laser diffraction. *Journal of Geophysical Research*, 113, C04023, doi:10.1029/2007JC004403
- Andersson, C.A., and R. Bro (2000). The N-way toolbox for MATLAB. *Chemometrics Intelligent Laboratory System* 52, 1–4.
- Carwardine, M. (1995). *Whales, Dolphins and Porpoises. A guide to all the world's cetaceans.* Eyewitness Handbooks. Doling Kindersley, London.
- Collier, R. (1984). Particulate and dissolved vanadium in the North Pacific Ocean. *Nature*, 309, 441-444.
- Collier, R. (1985). Molybdenum in the Northeast Pacific Ocean. *Limnol. Oceanogr.*, 30(6), 1351-1354.
- Emerson, S., & Husted, S. (1991). Ocean anoxia and the concentration of molybdenum and vanadium in seawater. *Marine Chemistry*, 34, 177-196.
- Firdaus, M.L. et al. (2007). Preconcentration of Zr, Hf, Nb, Ta and W in seawater using solid-phase extraction on TSK-8 hydroxyquinoline resin and determination by inductively coupled plasma-mass spectrometry. *Anal. Chim. Acta*, 583, 296–302.
- Firdaus, M., Norisuye, K., Nakagawa, Y., & Sohrin, Y. (2008). Dissolved and labile particulate Zr, Hf, Nb, Ta, Mo and W in the Western North Pacific Ocean. *J. Oceanogr.*, 64, 247-257.
- Godfrey, L., White, W., & Salters, V. (1996). Dissolved zirconium and hafnium distributions across a shelf break in the northeastern Atlantic Ocean. *Geochim. Cosmochim. Acta*, 60, 3995-4006.
- Goffart, P., Vandevivre & Massart, N. (2012). At sea distribution of seabirds and marine mammals: report to leg1 ANTXXVII.
- Gómez-Pereira, P.R., Fuchs, B.M., Alonso, C., Oliver, M.J., van Beusekom, J.E.E., Amann, R. (2010). Distinct flavobacterial communities in contrasting water masses of the North Atlantic Ocean. *ISME J* 4: 472–487.
- HELCOM (1988). *Guidelines for Baltic Monitoring Program.* Helsinki: Baltic Marine Environment Protection Commission, 116 pp.
- Helms, J.R., Stubbins, A., Ritchie, J.D.E., Minor, C., Kieber, D.J. & Mopper, K. (2008). Absorption spectral slopes and slope ratios as indicators of molecular weight, source, and photobleaching of chromophoric dissolved organic matter. *Limnology and Oceanography*, 53(3), 955–969.
- Henze, G.; *Polarographie und Voltammetrie – Grundlagen und analytische Praxis*; Springer-Verlag: Berlin Heidelberg, 2001.
- Hooker, S.B., Mobley, C.D., McLean, S., Holben, B., Miller, M., Pietras, C., Joiris, CR (1991). Spring distribution and ecological role of seabirds and marine mammals in the Weddell Sea, Antarctica. *Polar Biology*, 11, 415–424.

- Jaendel, C., Caisso, M., & Minster, J. (1987). Vanadium behavior in the global ocean and in Mediterranean Sea. *Marine Chemistry*, 21, 51-74.
- Joiris C.R., Falck, E. (2010). Summer at-sea distribution of Little Auks *Alle alle* and Harp Seals *Pagophilus (Phoca) groenlandica* in the Greenland Sea: impact of small-scale hydrological events. *Polar Biology*, 34, 541-548. DOI: 10.1007/s00300-010-0910-0. Online: 03 November 2010.
- Kaczmarek, S., D. Stramski, and M. Stramska (2003), The new pathlength amplification factor investigation, Abstract Publication 149, Baltic Sea Sciences Congress, Helsinki.
- Koschinsky, A., & Hein, J. (2003). Acquisition of elements from seawater by ferromanganese crusts: Solid phase associations and seawater speciation. *Marine Geology*, 198, 331-351.
- Kowalczyk P., Zabłocka, M., Sagan, S. & Kuliński, K. (2010). Fluorescence measured in situ as a proxy of CDOM absorption and DOC concentration in the Baltic Sea. *Oceanologia*, 52 (3), 431-471.
- Liu, S., Li, J., & Mao, X. (2003). Stripping Voltammetric determination of Zirconium with Complexing Preconcentration of Zirconium(IV) at a Mohrin-Modified Carbon Paste Electrode. *Electroanalysis*, 15, 1751-1755.
- Longhurst, Alan R., 2007: *Ecological Geography of the Sea*. Academic Press, 542p.
- Mary I., Heywood, J.L., Fuchs, B.M., Amann, R., Tarran, G.A., Burkill, P.H., Zubkov, M.V. (2006) SAR11 dominance among metabolically active low nucleic acid bacterioplankton in surface waters along an Atlantic meridional transect. *Aquat Microb Ecol* 45, 107-113.
- Middelburg, J., Hoede, D., Van der Sloot, H., Van der Weijden, C., & Wijkstra, J. (1988). Arsenic, antimony and vanadium in the North Atlantic Ocean. *Geochim. Cosmochim. Acta*, 52, 2871-2878.
- Morin, S., Savarino, J., Frey, M.M., Yan, N., Bekki, S., Bottenheim, J.W., Martins, J.M.F. (2008) Tracing the origin and fate of NO_x in the arctic atmosphere using stable isotopes in nitrate. *Science*, 322(5902), 730-732.
- Morin, S., Savarino, J., Frey, M.M., Domine, F., Jacobi, H.W., Kaleschke, L., Martins, J.M.F. (2009) Comprehensive isotopic composition of atmospheric nitrate in the Atlantic Ocean boundary layer from 65 degrees S to 79 degrees N, *Journal of Geophysical Research-Atmospheres*, 114.
- Mueller, J.L., Austin, R.W., Morel, A., Fargion, G.S. & McClain, C.R. (2003a). Ocean optics protocols for satellite ocean color sensor validation, Revision 4, Volume I: Introduction, background, and conventions. Greenbelt, MD: Goddard Space Flight Center. 50 p.
- Mueller, J.L., Pietras, C., Hooker, S.B., Austin, R.W., Miller, M., Knobelspiesse, K.D., Frouin, R., Holben, B. and Voss, K. (2003b). Ocean optics protocols for satellite ocean color sensor validation, Revision 4, Volume II: Instrument specifications, characterisation and calibration. Greenbelt, MD: Goddard Space Flight Center.
- Onley, D. & Scofield, P. (2007). *Albatross, Petrels and Shearwaters of the World*. Helm, London. 240 pp.
- Orians, K., Boyle, E., & Bruland, K. (1990). Dissolved titanium in the open ocean. *Nature*, 348, 322-325.
- Röckmann, T., Kaiser, J., Crowley, J.N., Brenninkmeijer, C.A.M., Crutzen, P.J. (2001) The origin of the anomalous or "mass-independent" oxygen isotope fractionation in tropospheric N₂O, *Geophysical Research Letters*, 28(3), 503-506.

- Savarino, J., Romero, A., Cole-Dai, J., Bekki, S., Thiemens, M.H. (2003) UV induced mass-independent sulfur isotope fractionation in stratospheric volcanic sulfate, *Geophysical Research Letters*, 30(21).
- Schotz, F. (1962). Pigmentanalytische untersuchungen an *Oenothera*. I. Vorversuche und analyse der blätter und blüten von *Oenothera suaveolens* Desf., Mutante 'wiesshers'. *Planta*, 58, 411 – 434.
- Schattenhofer, M., Fuchs, B.M., Amann, R., Zubkov, M.V., Tarran, G.A., Pernthaler, J. (2009) Latitudinal distribution of prokaryotic picoplankton populations in the Atlantic Ocean. *Environ Microbiol* 11: 2078–2093.
- Scholz, F.; *Electroanalytical Methods* ; Springer-Verlag Berlin Heidelberg ,2005.
- Sharp, J.H. 2002. Analytical methods for total DOM pools, p. 3558. In D. A. Hansell and C. A. Carlson [eds.], *Biogeochemistry of marine dissolved organic matter*. Academic Press.
- Shirihai, H. (2006). *Guide des mammifères marins du monde*. Delachaux et Niestle. 384 pp.
- Shirihai, H. (2008). *Birds and Marine Mammals of the Antarctic Continent and the Southern Ocean. The complete guide to Antarctic Wildlife*. Princeton University Press, Princeton & Oxford. 544 pp.
- Simon, M., Azam, F. (1989) Protein content and protein synthesis rates of planktonic marine bacteria. *Marine Ecology Progress Series* 51, 201-213.
- Simon, M., Rosenstock, B. (2007) Different coupling of dissolved amino acid, protein, and carbohydrate turnover to heterotrophic picoplankton production in the Southern Ocean in austral summer and fall. *Limnology and Oceanography* 52, 85-95.
- Skrabal, S. (2006). Dissolved titanium distributions in the Mid-Atlantic Bight. *Marine Chemistry*, 102, 218-229.
- Smith, R.C., & Baker, K.S. (1984). Analysis of ocean optical data, in *Ocean Optics VII*, edited by M. A. Blizard, *Proc. SPIE Int. Soc. Opt. Eng.*, vol. 489, pp. 119–126, Bellingham, WA.
- Sohrin, Y., Isshiki, L., Kuwamoto, T., & Nakayama, E. (1987). Tungsten in North Pacific waters. *Marine Chemistry*, 22, 95-102.
- Stedmon, C.A., Markager, S., Kaas, H., (2000). Optical properties and signatures of chromophoric dissolved organic matter (CDOM) in Danish coastal waters. *Estuarine, Coastal and Shelf Science* 51, 267–278.
- Stedmon, C.A., Markager, S. & Bro, R. (2003). Tracing dissolved organic matter in aquatic environments using a new approach to fluorescence spectroscopy. *Marine Chemistry* 82, 239–254.
- Stedmon, C.A. & Bro, R. (2008). Characterizing dissolved organic matter fluorescence with parallel factor analysis: a tutorial. *Limnology and Oceanography: Methods* 6, 572–579.
- Tassan, S., and Ferrari, G.M. (1995), An alternative approach to absorption measurements of aquatic particles retained on filters, *Limnology and Oceanography*, 40, 1358– 1368.
- Wang, D., Aller, R., & Sanudo-Wilhelmy. (2009). A method for the quantification of different redox-species of molybdenum (V and VI) in seawater. *Marine Chemistry*, 113, 250-256.
- Vicars, W.C., Bhattacharya, S.K., Erbland, J., Savarino, J. (2012) Measurement of the ^{17}O -excess of tropospheric ozone using a nitrite-coated filter, *Rapid Communications in Mass Spectrometry*, 26, 1-13.

Zaneveld, J.R.V., Kitchen, J.C. & Moore, C. (1994). The scattering error correction of reflecting-tube absorption meters, *Ocean Optics XII, Proc. SPIE*, 2258, 44–55.

Zubkov, M., Tarran, G.A., Mayr, I., Fuchs, B.M. (2008) Differential microbial uptake of dissolved amino acids and amino sugars in surface waters of the Atlantic Ocean. *J Plankton Res* 30, 211-220.

APPENDIX

A.1 Teilnehmende Institute/participating institutions

A.2 Fahrtteilnehmer/cruise participants

A.3 Schiffsbesatzung/ship's crew

A.4 Stationsliste/station list

A.1 TEILNEHMENDE INSTITUTE / PARTICIPATING INSTITUTIONS

Institut / Institute	Adresse / Address
Atlas	ATLAS HYDROGRAPHIC GmbH Kurfürstenallee 130 28211 Bremen/Germany
AWI	Stiftung Alfred-Wegener-Institut für Polar- und Meeresforschung in der Helmholtz-Gemeinschaft Am Handelshafen 12 27570 Bremerhaven/Germany
DWD	Deutscher Wetterdienst Geschäftsbereich Wettervorhersage Schiffahrtsberatung Bernhard-Nocht-Str. 76 20359 Hamburg/Germany
HZI	Helmholtz-Zentrum für Infektionsfor- schung GmbH Inhoffenstraße 7 38124 Braunschweig/Germany
IAU	Institut für Atmosphäre und Umwelt- Altenhöferallee 1 60438 Frankfurt/Main /Germany
ICBM	Institut für Chemie und Biologie des Meeres Carl-von-Ossietzky-Str. 9-11 26111 Oldenburg/Germany
Förderverein Auricher Wissenschaftstage	Förderverein Auricher Wissenschaftstage Gaußstr. 18 26603 Aurich/Germany
GEOMAR	Helmholtz-Centre for Ocean Research Düsternbrooker Weg 20 24105 Kiel/Germany
Ift	Institute for Tropospheric Research Permoserstr. 15 04318 Leipzig/Germany

Institut / Institute	Adresse / Address
IOPAS	Institute of Oceanology Polish Academy of Science Ul. Powstańców Warszawy 55 81-712 Sopot/Poland
Jacobs University	Jacobs University Campus Ring 1 28759 Bremen/Germany
Johannes Althusius Gymnasium	Johannes Althusius Gymnasium Früchteburger Weg 28 26721 Emden
LGGE	Laboratoire de Glaciologie et Géophysique de l'Environnement (UMR 5183) 54 rue Molière 38402 - Saint Martin d'Hères cedex / France
LIM	Universität Leipzig Fakultät für Physik und Geowissenschaften Leipziger Institut für Meteorologie Stephanstr. 3 04103 Leipzig /Germany
MPI	Max-Planck-Institut für Meteorologie Bundesstr. 53 20146 Hamburg/Germany
PoIE	Belgian Laboratory for Polar Ecology Rue du Fodia B-1367 Ramillies/Belgium
Uni GÖ	Georg-August-Universität Göttingen Wilhelmsplatz 1 37073 Göttingen/Germany

A.2 FAHRTTEILNEHMER / CRUISE PARTICIPANTS

Name / Last Name	Vorname / First Name	Institut/ Institute	Beruf/ Profession
Assmann	Denise	IfT	Student, Meteorology
Batista Schneider	Alexandre	Jacobs University	PhD-student, chemistry
Betti	Paola	Observer of Argentina	Biologist
Beudels-Jamar	Roselin	PolE	Biologist
Billerbek	Sara	ICBM	PhD student, micro-biology
Brückner	Marlen	IfT	Meteorologist
Bumke	Karl	IFM-GEOMAR	Meteorologist
Chellappan	Seethala	MPI	Meteorologist
Eckel	Felix	Johannes- Althusius- Gymnasium Emden	Pupil
El Naggar	Saad	AWI	Physicist
Ewert	Jörn	Atlas	Engineer
Fritz	Lea	Förderverein Auricher Wissenschaftstage	Pupil
Fuchs	Susanne	IfT	Technician
Gerchow	Peter	AWI	Engineer
Giebel	Helge A.	ICBM	Microbiologist
Glowacki	Oskar	IOPAS	Student, oceanography
Gavrilov	Alexander	ICBM	Student assistant
Hartmann	Susan	IfT	Technican
Hempelt	Juliane	DWD	Weather-Technican
Henschel	Anke	Förderverein Auricher Wissenschaftstage	Teacher
Höpner	Friederike	IfT	PhD-student, meteorolog
Huang	Shan	IfT	Meteorologist
Immerz	Antonia	AWI	Technican
Jamar de Bolsée	Oria	PolE	Geographer
Kohn	Monika	Uni Gö	Student, meteorology
Koschnik	Nils	AWI	Engineer
Kowalczuk	Piotr	IOPAS	Oceanographer
Krocker	Ralf	AWI	Engineer

A.2 Cruise participants

Name / Last Name	Vorname / First Name	Institut/ Institute	Beruf/ Profession
Lafontaine	René-Marie	PolE	Biologist
Leistert	Michael	IfT	Student, meteorology
Loewen	Pauline	Förderverein Auricher Wissenschaftstage	Pupil
Merkel	Maik	IfT	Meteorologist
Miller	Max	DWD	Meteorologist
Rackebrandt	Siri	ICBM	Student, Environmental Science
Raczkowska	Anna	IOPAS	Student, oceanography
Remke	Thomas	ICBM	Student, marine environmental science
Sagan	Slawomir	IOPAS	Oceanographer
Sandersfeld	Tina	AWI	Student, biology
Schäfer	Michael	LIM	Meteorologist
Schneider	Alexandre Batista	Jacobs Uni	PhD Student, chemistry
Seibt	Maren	ICBM	PhD Student, geochemistry
Simon	Meinhard	ICBM	Microbiologist
Stumm	Maren	ICBM	Biologist
Ungermann	René	ICBM	PhD Student, geochemistry
Vicars	William	LGGE	PhD Student, environmental science
Vollmers	John	Uni GÖ	PhD Student, micro-biology
Wagner-Döbler	Irene	HZI	Microbiologist
Wang	Hui	HZI	PhD Student, micro-biology
Wietz	Matthias	AWI	Scientist
Wurst	Mascha	ICBM	PhD Student, micro-biology
Wurz	Erik	AWI	Student
Zablocka	Monika	IOPAS	Oceanographer

A.3 SCHIFFSBESATZUNG /SHIP'S CREW

No.	Name	Rank
1	Pahl, Uwe	Master
2	Spielke, Steffen	1. Offc.
3	Ziemann, Olaf	Ch. Eng.
4	Hering, Igor	2. Offc.
5	Peine, Lutz	2. Offc. 3. Offc.
6	Birkner, Thomas	Doctor
7	Koch, Georg	R. Offc.
8	Kotnik, Herbert	2. Eng.
9	Schnürch, Helmut	2. Eng.
10	Westphahl, Henning	2. Eng.
11	Brehme, Andreas	Elec. Eng.
12	Feiertag, Thomas	ELO
13	Fröb, Martin	ELO
14	Muhle, Helmut	ELO
15	Winter, Andreas	ELO
16	Clasen, Burkhard	Boatsw.
17	Neisner, Winfried	Carpenter
18	Burzan, Gerd-Ekkeh.	A.B.
19	Hartwig-Lab., Andreas	A.B.
20	Kreis, Reinhard	A.B.
21	Kretschmar, Uwe	A.B.
22	Moser, Siegfried	A.B.
23	Schröder, Norbert	A.B.
24	Schröter, René	A.B.
25	Schultz, Ottomar	A.B.
26	Beth, Detlef	Storek.
27	Becker, Holger	Mot-man
28	Dinse, Horst	Mot-man
29	Fritz, Günter	Mot-man
30	Krösche, Eckrad	Mot-man

31	Watzel, Bernhard	Mot-man
32	Fischer, Matthias	Cook
33	Martens, Michael	Cooksmate
34	Tupy, Mario	Cooksmate
35	Dinse, Petra	1. Stwdess
36	Hennig, Christina	Stwdess/N.
37	Chen, Quan Lun	2. Stwdess
38	Hischke, Peggy	2. Steward
39	Hu, Guo Yong	2. Stwdess
40	Streit, Christina	2. Steward
41	Wartenberg, Irena	2. Stwdess
42	Ruan, Hui Guang	Laundrym.

A.4 STATIONSLISTE/STATION LIST PS 79

Station	Date	Time	Gear	Action	Position Lat	Position Lon	Water depth (m)
PS79/296-1	11.04.2012	17:02:00	UWRAD	on ground/max depth	51° 3,32' S	66° 27,80' W	50
PS79/296-2	11.04.2012	17:06:00	CTD/RO	on ground/max depth	51° 3,34' S	66° 27,80' W	109
PS79/296-3	11.04.2012	17:43:00	CTD/RO	on ground/max depth	51° 3,22' S	66° 27,56' W	103
PS79/297-1	12.04.2012	17:12:00	UWRAD	on ground/max depth	47° 56,40' S	61° 55,22' W	50
PS79/297-2	12.04.2012	17:13:00	CTD/RO	on ground/max depth	47° 56,41' S	61° 55,23' W	19
PS79/297-3	12.04.2012	17:33:00	CTD/RO	on ground/max depth	47°56,47' S	61° 55,36' W	140
PS79/298-1	13.04.2012	16:14:00	CTD/RO	on ground/max depth	45° 5,66' S	58° 9,81' W	203
PS79/298-2	13.04.2012	16:32:00	UWRAD	on ground/max depth	45° 5,68' S	58° 9,74' W	50
PS79/298-3	13.04.2012	17:57:00	CTD/RO	on ground/max depth	45° 5,57' S	58° 9,73' W	2971
PS79/298-4	13.04.2012	19:23:00	OS	on ground/max depth	45° 5,47' S	58° 9,70' W	50
PS79/299-1	14.04.2012	16:02:00	UWRAD	on ground/max depth	42° 49,42' S	54° 37,79' W	5352
PS79/299-2	14.04.2012	16:14:00	CTD/RO	on ground/max depth	42° 49,48' S	54° 37,68' W	204
PS79/299-3	14.04.2012	16:39:00	OS	on ground/max depth	42° 49,58' S	54° 37,43' W	200
PS79/300-1	15.04.2012	16:03:00	UWRAD	on ground/max depth	39° 48,02' S	50° 35,15' W	50
PS79/300-2	15.04.2012	16:14:00	CTD/RO	on ground/max depth	39° 48,01' S	50° 35,07' W	203
PS79/300-3	15.04.2012	16:45:00	OS	on ground/max depth	39° 47,99' S	50° 34,90' W	200
PS79/300-4	15.04.2012	17:15:00	CTD/RO	on ground/max depth	39° 47,89' S	50° 34,62' W	204
PS79/301-1	16.04.2012	15:05:00	UWRAD	on ground/max depth	37° 5,05' S	46° 51,02' W	50
PS79/301-2	16.04.2012	15:18:00	OS	on ground/max depth	37° 5,00' S	46° 51,07' W	200
PS79/301-3	16.04.2012	16:23:00	CTD/RO	on ground/max depth	37° 5,11' S	46° 51,26' W	2143
PS79/302-1	17.04.2012	15:04:00	UWRAD	on ground/max depth	34° 14,36' S	42° 58,14' W	50
PS79/302-2	17.04.2012	15:17:00	CTD/RO	on ground/max depth	34° 14,33' S	42° 58,05' W	203
PS79/302-3	17.04.2012	15:50:00	OS	on ground/max depth	34° 14,27' S	42° 57,89' W	200
PS79/302-4	17.04.2012	16:17:00	CTD/RO	on ground/max depth	34° 14,31' S	42° 57,90' W	201
PS79/303-1	18.04.2012	15:03:00	UWRAD	on ground/max depth	31° 18,38' S	39° 18,82' W	50
PS79/303-2	18.04.2012	15:16:00	CTD/RO	on ground/max depth	31° 18,36' S	39° 18,83' W	202
PS79/303-3	18.04.2012	15:44:00	OS	on ground/max depth	31° 18,36' S	39° 18,86' W	200
PS79/304-1	18.04.2012	18:52:00	CTD/RO	on ground/max depth	30° 59,95' S	38° 59,69' W	200
PS79/305-1	19.04.2012	14:03:00	UWRAD	on ground/max depth	28° 5,55' S	38° 59,92' W	50
PS79/306-1	20.04.2012	02:11:00	CTD/RO	on ground/max depth	25° 59,90' S	39° 0,04' W	204
PS79/306-2	20.04.2012	04:21:00	CTD/RO	on ground/max depth	25° 59,99' S	39° 0,04' W	4100
PS79/307-1	20.04.2012	14:03:00	UWRAD	on ground/max depth	24° 45,19' S	38° 0,97' W	50
PS79/307-2	20.04.2012	14:14:00	CTD/RO	on ground/max depth	24° 45,24' S	38° 1,03' W	203

A.4 Station list PS 79

Station	Date	Time	Gear	Action	Position Lat	Position Lon	Water depth (m)
PS79/307-3	20.04.2012	14:40:00	OS	on ground/max depth	24° 45,29' S	38° 1,06' W	200
PS79/307-4	20.04.2012	15:07:00	CTD/RO	on ground/max depth	24° 45,22' S	38° 1,10' W	204
PS79/308-1	21.04.2012	13:12:00	OS	on ground/max depth	21° 13,80' S	35° 24,20' W	200
PS79/308-2	21.04.2012	14:48:00	CTD/RO	on ground/max depth	21° 13,76' S	35° 24,12' W	4080
PS79/308-3	21.04.2012	14:02:00	UWRAD	on ground/max depth	21° 13,81' S	35° 24,18' W	50
PS79/309-1	21.04.2012	21:12:00	HS_PS	profile start	20° 40,29' S	35° 1,96' W	2179
PS79/309-1	22.04.2012	00:23:59	HS_PS	profile end	20° 40,28' S	34° 57,03' W	91
PS79/310-1	22.04.2012	14:05:00	UWRAD	on ground/max depth	18° 38,73' S	33° 43,78' W	50
PS79/310-2	22.04.2012	14:15:00	CTD/RO	on ground/max depth	18° 38,73' S	33° 43,79' W	202
PS79/310-3	22.04.2012	14:42:00	OS	on ground/max depth	18° 38,74' S	33° 43,82' W	200
PS79/310-4	22.04.2012	16:47:00	CTD/RO	on ground/max depth	18° 39,81' S	33° 43,52' W	4362
PS79/311-1	23.04.2012	14:03:00	UWRAD	on ground/max depth	15° 31,29' S	31° 51,69' W	50
PS79/311-2	23.04.2012	14:14:00	CTD/RO	on ground/max depth	15° 31,30' S	31° 51,69' W	204
PS79/311-3	23.04.2012	14:46:00	OS	on ground/max depth	15° 31,35' S	31° 51,74' W	200
PS79/312-1	24.04.2012	14:06:00	UWRAD	on ground/max depth	11° 53,85' S	29° 45,09' W	50
PS79/312-2	24.04.2012	14:18:00	CTD/RO	on ground/max depth	11° 53,87' S	29° 45,08' W	203
PS79/312-3	24.04.2012	14:44:00	OS	on ground/max depth	11° 53,86' S	29° 45,11' W	200
PS79/312-4	24.04.2012	15:08:00	CTD/RO	on ground/max depth	11° 53,86' S	29° 45,09' W	203
PS79/313-1	25.04.2012	14:19:00	CTD/RO	on ground/max depth	8° 12,68' S	27° 59,48' W	204
PS79/313-2	25.04.2012	14:38:00	UWRAD	on ground/max depth	8° 12,75' S	27° 59,48' W	50
PS79/313-3	25.04.2012	14:47:00	OS	on ground/max depth	8° 12,77' S	27° 59,47' W	200
PS79/313-4	25.04.2012	15:19:00	CTD/RO	on ground/max depth	8° 12,87' S	27° 59,53' W	203
PS79/314-1	26.04.2012	11:46:00	UWRAD	on ground/max depth	5° 5,94' S	26° 38,52' W	50
PS79/314-2	26.04.2012	11:21:00	CTD/RO	on ground/max depth	5° 5,83' S	26° 38,34' W	211
PS79/314-3	26.04.2012	11:59:00	OS	on ground/max depth	5° 5,91' S	26° 38,53' W	202
PS79/314-4	26.04.2012	14:10:00	CTD/RO	on ground/max depth	5° 6,00' S	26° 38,66' W	5747
PS79/315-1	27.04.2012	14:07:00	UWRAD	on ground/max depth	1° 29,36' S	25° 19,31' W	50
PS79/315-2	27.04.2012	14:17:00	CTD/RO	on ground/max depth	1° 29,32' S	25° 19,27' W	203
PS79/315-3	27.04.2012	14:44:00	OS	on ground/max depth	1° 29,23' S	25° 19,19' W	200
PS79/315-4	27.04.2012	15:08:00	CTD/RO	on ground/max depth	1° 29,19' S	25° 19,08' W	203
PS79/316-1	28.04.2012	08:12:00	HS_PS	profile start	1° 27,83' N	24° 21,92' W	2701
PS79/316-1	28.04.2012	11:34:59	HS_PS	profile end	1° 27,77' N	24° 22,08' W	2723
PS79/317-1	29.04.2012	14:04:00	UWRAD	on ground/max depth	6° 3,57' N	23° 28,93' W	50
PS79/317-2	29.04.2012	14:16:00	CTD/RO	on ground/max depth	6° 3,54' N	23° 28,90' W	203
PS79/317-3	29.04.2012	14:51:00	OS	on ground/max depth	6° 3,53' N	23° 28,85' W	200

A.4 Station list PS 79

Station	Date	Time	Gear	Action	Position Lat	Position Lon	Water depth (m)
PS79/317-4	29.04.2012	16:27:00	CTD/RO	on ground/max depth	6° 3,56' N	23° 28,84' W	4280
PS79/318-1	30.04.2012	13:03:00	UWRAD	on ground/max depth	9° 24,48' N	22° 46,40' W	50
PS79/318-2	30.04.2012	13:15:00	CTD/RO	on ground/max depth	9° 24,45' N	22° 46,33' W	203
PS79/318-3	30.04.2012	13:50:00	OS	on ground/max depth	9° 24,40' N	22° 46,32' W	200
PS79/318-4	30.04.2012	15:25:00	CTD/RO	on ground/max depth	9° 24,42' N	22° 46,39' W	4076
PS79/319-1	01.05.2012	13:09:00	UWRAD	on ground/max depth	12° 35,39' N	22° 11,71' W	50
PS79/319-2	01.05.2012	13:18:00	CTD/RO	on ground/max depth	12° 35,39' N	22° 11,73' W	202
PS79/319-3	01.05.2012	13:42:00	OS	on ground/max depth	12° 35,35' N	22° 11,73' W	200
PS79/319-4	01.05.2012	15:19:00	CTD/RO	on ground/max depth	12° 35,11' N	22° 11,66' W	4075
PS79/320-1	02.05.2012	13:15:00	CTD/RO	on ground/max depth	16° 54,29' N	21° 34,09' W	203
PS79/320-2	02.05.2012	13:42:00	OS	on ground/max depth	16° 54,25' N	21° 34,10' W	200
PS79/320-3	02.05.2012	14:03:00	CTD/RO	on ground/max depth	16° 54,26' N	21° 34,11' W	202
PS79/321-1	03.05.2012	12:07:00	UWRAD	on ground/max depth	20° 42,29' N	21° 10,32' W	50
PS79/321-2	03.05.2012	12:07:00	CTD/RO	on ground/max depth	20° 42,29' N	21° 10,32' W	20
PS79/321-3	03.05.2012	12:26:00	OS	on ground/max depth	20° 42,33' N	21° 10,27' W	200
PS79/321-4	03.05.2012	12:54:00	CTD/RO	on ground/max depth	20° 42,28' N	21° 10,20' W	203
PS79/322-1	04.05.2012	12:18:00	CTD/RO	on ground/max depth	24° 23,75' N	19° 52,05' W	203
PS79/322-2	04.05.2012	12:45:00	OS	on ground/max depth	24° 23,79' N	19° 52,06' W	200
PS79/322-3	04.05.2012	13:06:00	UWRAD	on ground/max depth	24° 23,84' N	19° 51,97' W	50
PS79/322-4	04.05.2012	14:18:00	CTD/RO	on ground/max depth	24° 23,99' N	19° 51,81' W	3672
PS79/323-1	05.05.2012	12:05:00	UWRAD	on ground/max depth	26° 20,88' N	17° 18,70' W	50
PS79/323-2	05.05.2012	12:17:00	CTD/RO	on ground/max depth	26° 20,89' N	17° 18,72' W	202
PS79/323-3	05.05.2012	12:45:00	OS	on ground/max depth	26° 20,94' N	17° 18,77' W	200
PS79/324-1	07.05.2012	12:01:00	UWRAD	on ground/max depth	33° 23,96' N	13° 31,99' W	50
PS79/324-2	07.05.2012	12:16:00	CTD/RO	on ground/max depth	33° 23,95' N	13° 32,03' W	205
PS79/324-3	07.05.2012	12:49:00	OS	on ground/max depth	33° 23,94' N	13° 32,10' W	200
PS79/324-4	07.05.2012	13:15:00	CTD/RO	on ground/max depth	33° 23,87' N	13° 32,06' W	205
PS79/325-1	07.05.2012	22:50:00	HS_PS	profile start	35° 5,99' N	13° 2,03' W	1809
PS79/325-1	07.05.2012	23:49:00	HS_PS	profile end	35° 3,01' N	12° 53,96' W	142
PS79/325-1	08.05.2012	00:03:00	HS_PS	profile start	35° 3,02' N	12° 54,00' W	143
PS79/325-1	08.05.2012	01:09:00	HS_PS	profile end	35° 6,01' N	13° 1,98' W	1787
PS79/325-1	08.05.2012	01:21:00	HS_PS	profile start	35° 6,05' N	13° 2,07' W	1838
PS79/325-1	08.05.2012	02:22:00	HS_PS	profile end	35° 2,98' N	12° 53,95' W	167
PS79/325-1	08.05.2012	02:39:00	HS_PS	profile start	35° 2,92' N	12° 53,88' W	142

A.4 Station list PS 79

Station	Date	Time	Gear	Action	Position Lat	Position Lon	Water depth (m)
PS79/325-1	08.05.2012	03:42:00	HS_PS	profile end	35° 5,96' N	13° 1,89' W	1750
PS79/325-1	08.05.2012	03:54:00	HS_PS	profile start	35° 6,01' N	13° 2,04' W	1812
PS79/325-1	08.05.2012	04:55:00	HS_PS	profile end	35° 3,01' N	12° 54,04' W	146
PS79/325-1	08.05.2012	05:04:00	HS_PS	profile start	35° 2,84' N	12° 53,78' W	138
PS79/325-1	08.05.2012	06:05:00	HS_PS	profile end	35° 6,01' N	13° 1,99' W	1784
PS79/325-1	08.05.2012	06:17:00	HS_PS	profile start	35° 6,02' N	13° 2,05' W	1819
PS79/325-1	08.05.2012	07:19:00	HS_PS	profile end	35° 3,03' N	12° 54,08' W	144
PS79/325-1	08.05.2012	09:09:59	HS_PS	profile end	35° 14,45' N	12° 54,54' W	2895
PS79/326-1	08.05.2012	09:39:00	CTD/RO	on ground/max depth	35° 14,32' N	12° 53,84' W	202
PS79/326-2	08.05.2012	11:18:00	CTD/RO	on ground/max depth	35° 14,27' N	12° 53,69' W	2820
PS79/326-3	08.05.2012	10:33:00	UWRAD	on ground/max depth	35° 14,24' N	12° 53,65' W	50
PS79/326-4	08.05.2012	12:42:00	OS	on ground/max depth	35° 14,33' N	12° 53,55' W	200
PS79/327-1	08.05.2012	13:48:00	HS_PS	profile start	35° 12,99' N	13° 2,95' W	2571
PS79/327-1	08.05.2012	15:51:59	HS_PS	profile end	35° 19,03' N	13° 19,10' W	4819
PS79/328-1	09.05.2012	09:14:00	CTD/RO	on ground/max depth	38° 44,70' N	12° 36,53' W	202
PS79/328-2	09.05.2012	09:42:00	OS	on ground/max depth	38° 44,77' N	12° 36,55' W	200
PS79/328-3	09.05.2012	11:18:00	CTD/RO	on ground/max depth	38° 44,80' N	12° 36,59' W	4074
PS79/328-4	09.05.2012	11:04:00	UWRAD	on ground/max depth	38° 44,82' N	12° 36,62' W	50
PS79/329-1	10.05.2012	11:09:00	UWRAD	on ground/max depth	43° 2,65' N	10° 56,14' W	50
PS79/329-2	10.05.2012	11:19:00	CTD/RO	on ground/max depth	43° 2,59' N	10° 56,15' W	203
PS79/329-3	10.05.2012	11:45:00	OS	on ground/max depth	43° 2,58' N	10° 56,15' W	200
PS79/329-4	10.05.2012	12:10:00	CTD/RO	on ground/max depth	43° 2,54' N	10° 56,10' W	203
PS79/330-1	11.05.2012	11:05:00	UWRAD	on ground/max depth	47° 2,62' N	8° 5,44' W	50
PS79/330-2	11.05.2012	11:15:00	CTD/RO	on ground/max depth	47° 2,63' N	8° 5,43' W	203
PS79/330-3	11.05.2012	11:46:00	OS	on ground/max depth	47° 2,68' N	8° 5,44' W	200

Die "**Berichte zur Polar- und Meeresforschung**" (ISSN 1866-3192) werden beginnend mit dem Heft Nr. 569 (2008) als Open-Access-Publikation herausgegeben. Ein Verzeichnis aller Hefte einschließlich der Druckausgaben (Heft 377-568) sowie der früheren "**Berichte zur Polarforschung**" (Heft 1-376, von 1981 bis 2000) befindet sich im open access institutional repository for publications and presentations (**ePIC**) des AWI unter der URL <http://epic.awi.de>. Durch Auswahl "Reports on Polar- and Marine Research" (via "browse"/"type") wird eine Liste der Publikationen sortiert nach Heftnummer innerhalb der absteigenden chronologischen Reihenfolge der Jahrgänge erzeugt.

To generate a list of all Reports past issues, use the following URL: <http://epic.awi.de> and select "browse"/"type" to browse "Reports on Polar and Marine Research". A chronological list in declining order, issues chronological, will be produced, and pdf-icons shown for open access download.

Verzeichnis der zuletzt erschienenen Hefte:

Heft-Nr. 642/2012 — "Russian-German Cooperation SYSTEM LAPTEV SEA: The Expedition LENA 2008", edited by Dirk Wagner, Paul Overduin, Mikhail N. Grigoriev, Christian Knoblauch, and Dimitry Yu. Bolshiyarov

Heft-Nr. 643/2012 — "The Expedition of the Research Vessel 'Sonne' to the subpolar North Pacific and the Bering Sea in 2009 (SO202-INOPEX)", edited by Rainer Gersonde

Heft-Nr. 644/2012 — "The Expedition of the Research Vessel 'Polarstern' to the Antarctic in 2011 (ANT-XXVII/3)", edited by Rainer Knust, Dieter Gerdes and Katja Mintenbeck

Heft-Nr. 645/2012 — "The Expedition of the Research Vessel 'Polarstern' to the Arctic in 2011 (ARK-XXVI/2)", edited by Michael Klages

Heft-Nr. 646/2012 — "The Expedition of the Research Vessel 'Polarstern' to the Antarctic in 2011/12 (ANT-XXVIII/2)", edited by Gerhard Kattner

Heft-Nr. 647/2012 — "The Expedition of the Research Vessel 'Polarstern' to the Arctic in 2011 (ARK-XXVI/1)", edited by Agnieszka Beszczynska-Möller

Heft-Nr. 648/2012 — "Interannual and decadal variability of sea ice drift, concentration and thickness in the Weddell Sea", by Sandra Schwegmann

Heft-Nr. 649/2012 — "The Expedition of the Research Vessel 'Polarstern' to the Arctic in 2011 (ARK-XXVI/3 - TransArc)", edited by Ursula Schauer

Heft-Nr. 650/2012 — "Combining stationary Ocean Models and mean dynamic Topography Data", by Grit Freiwald

Heft-Nr. 651/2012 — "Phlorotannins as UV-protective substances in early developmental stages of brown algae", by Franciska S. Steinhoff

Heft-Nr. 652/2012 — "The Expedition of the Research Vessel 'Polarstern' to the Antarctic in 2012 (ANT-XXVIII/4)", edited by Magnus Lucassen

Heft-Nr. 653/2012 — "Joint Russian-German Polygon Project East Siberia 2011 - 2014: The expedition Kytalyk 2011", edited by Lutz Schirrmeister, Lyudmila Pestryakova, Sebastian Wetterich and Vladimir Tumskoy

Heft-Nr. 654/2012 — "The Expedition of the Research Vessel 'Polarstern' to the Antarctic in 2012 (ANT-XXVIII/5)", edited by Karl Bumke